NUREG/CR-5591
ORNL/TM-11568/V6&N1
Vol. 6, No. 1

Heavy-Section Steel Irradiation Program

Progress Report for
October 1994 – March 1995

Manuscript Completed: August 1995
Date Published: October 1995

Prepared by
W. R. Corwin

Oak Ridge National Laboratory
Operated by Martin Marietta Energy Systems, Inc.

Oak Ridge National Laboratory
Oak Ridge, TN 37831-6285

M. G. Vassilaros, NRC Project Manager

Prepared for
Division of Engineering Technology
Office of Nuclear Regulatory Research
U.S. Nuclear Regulatory Commission
Washington, DC 20555-0001
NRC Job Code L1098

Abstract

Maintaining the integrity of the reactor pressure vessel (RPV) in a light-water-cooled nuclear power plant is crucial in preventing and controlling severe accidents which have the potential for major contamination release. The RPV is the only key safety-related component of the plant for which a duplicate or redundant backup system does not exist. It is therefore imperative to understand and be able to predict the capabilities and limitations of the integrity inherent in the RPV. In particular, it is vital to fully understand the degree of irradiation-induced degradation of the RPV's fracture resistance which occurs during service, since without that radiation damage, it is virtually impossible to postulate a realistic scenario that would result in RPV failure.

For this reason, the Heavy-Section Steel Irradiation (HSSI) Program has been established with its primary goal to provide a thorough, quantitative assessment of the effects of neutron irradiation on the material behavior and, in particular, the fracture toughness properties of typical pressure-vessel steels as they relate to light-water RPV integrity. Effects of specimen size; material chemistry; product form and microstructure; irradiation fluence, flux, temperature, and spectrum; and postirradiation annealing are being examined on a wide range of fracture properties. The HSSI Program is arranged into 14 tasks: (1) program management, (2) fracture toughness curve shift in high-copper weldments (Series 5 and 6), (3) K_{Ic} and K_{Ia} curve shifts in low upper-shelf (LUS) welds (Series 8), (4) irradiation effects in a commercial LUS weld (Series 10), (5) irradiation effects on weld heat-affected zone (HAZ) and plate materials (Series 11), (6) annealing effects in LUS welds (Series 9), (7) microstructural and microfracture analysis of irradiation effects, (8) in-service irradiated and aged material evaluations, (9) Japan Power Development Reactor (JPDR) steel examination, (10) fracture toughness curve shift method, (11) special technical assistance, (12) technical assistance for Joint Coordinating Committee on Civilian Nuclear Reactor Safety (JCCCNRS) Working Groups 3 and 12, (13) correlation monitor materials, and (14) test reactor coordination.

During this period, the test results of the Italian crack-arrest specimens were analyzed and preparation of a NUREG report begun. The fabrication of two of the three trial LUS scoping welds to identify possible materials for studies on K_{Ic} shifts in LUS materials was completed and the third begun. Data from fracture mechanics testing of the irradiated LUS Midland Weld WF-70 were used to benchmark American Society of Mechanical Engineers (ASME) methods currently in use. The ASME lower-bound K_{Ic} curves were shown to be very conservative. The 5% lower-bound curve on the master curve, offset by only a 10°C margin, bounds the experimental data more accurately. Estimates of crack-arrest shifts were made from autographic load-time traces during the standard Charpy V-notch (CVN) impact tests. For the WF-70 beltline weld metal, the shift in K_{Ia} transition temperature derived from Charpy tests appears to be only one-half of the 41-J transition temperature shift. Large specimens are available to check this result. Precracked Charpy specimens, tested as fracture mechanics three-point bend bars, were used in conjunction with the proposed American Society for Testing and Materials (ASTM) master curve test practice currently under development to obtain T_o reference temperatures from both beltline and nozzle course weld metals before and after irradiation at 1×10^{19} neutrons/cm^2. The results from beltline weld metal were compatible with the results from larger fracture mechanics specimens. However, the lower initial toughness of the nozzle course material was not indicated by the Charpy specimens. The second large Midland irradiation capsule, 10.06, was shipped to Oak Ridge National Laboratory (ORNL) from the Ford Nuclear Reactor (FNR). A preliminary report on the exposure parameters for the first large capsule, 10.05 [1×10^{19} neutrons/cm^2 (< 1 MeV)], was prepared and is undergoing internal peer review. Two plates were identified for examination of the effects of neutron irradiation on the fracture toughness of the HAZ of welds of A 302 grade B (A302B) plate materials typical of those used in fabricating older RPVs. Arrangements are being made with Yankee Atomic Electric Company for procurement of the plates. Effects of annealing on the CVN impact energy specimens from the LUS welds from the Midland beltline and nozzle course welds, as well as Heavy-Section Steel Technology (HSST) plate 02 and HSSI weld 73W, were examined as was the effect of annealing on the initiation fracture toughness of annealed material from Midland beltline weld and HSST plate 02. The fabrication of major components for the irradiation, annealing, and reirradiation (IAR) facility for the first two positions of the FNR at the University of Michigan was begun as were the temperature and dosimetry verification capsules. The design of a reusable capsule capable of reirradiating previously irradiated and annealed CVN and 1T C(T) specimens was partly completed. The data acquisition and control instrumentation for the first two IAR facilities were essentially completed. Characterization of long-term (~100,000 h) thermally aged and neutron-irradiated surveillance materials by atom-probe field-ion microscopy indicated that thermal aging did not result in any copper clustering or

compositional changes in the ferrite matrix. A comparison with the as-fabricated welds verified that copper precipitation during the postweld heat treatment had reduced the matrix copper content below the nominal bulk value. Analysis of ion-irradiated model alloys has demonstrated the role of point defect clusters in hardening, and a preliminary microstructure/hardening correlation was obtained. A significant body of French pressurized-water reactor surveillance data has been obtained and formatted for comparison with U.S. data and for use in calibrating kinetic embrittlement models. Preparations were made for hot cell installation of the recently acquired computer numerically controlled machining center. Tensile, CVN, and fracture toughness testing of three-wire stainless steel cladding, thermally aged for 20,000 h at 288 or at 343°C, was completed and a draft report was prepared, showing that the effects of thermal aging at either temperature were very small. Tensile tests of type 308 stainless steel weld metal, aged at 343°C for 50,000 h, showed that aging has little effect on the tensile properties. Work was virtually concluded to evaluate the existing neutron dosimetry and transport calculations which have been performed for the JPDR by the Japanese as well as to perform similar transport calculations at ORNL. The ORNL transport calculations included the concrete in the biological shield as well as the pressure vessel. All currently available fracture toughness data bases were analyzed, and it was shown that, on average, the fracture toughness shifts generally exceeded the Charpy 41-J shifts; a linear least-squares fit to the data set yielded a slope of 1.15. The observed dissimilarity was analyzed by taking into account differences in effects of irradiation on Charpy impact and fracture toughness properties. Based on these comparisons, a procedure to adjust Charpy 41-J shifts for achieving a more reliable correlation with the fracture toughness shifts was evaluated. SRI completed initial testing of notched round bar specimens fabricated from weld 72W material. The notched round bar results agree well with the 1T compact data in the middle of the transition regime but tend to show higher toughness than the 1T specimens at lower test temperatures. Explorations into the reasons for the difference are being pursued. A draft report describing the testing of subsize Charpy specimens has been written describing a new approach to normalizing data from subsize specimens. This method gives excellent agreement with the data from full-size specimens for materials that have LUS levels less than about 200 J. All of the reconstituted Charpy specimens have been tested for the ASTM round robin and the results tabulated and transmitted to ASTM for their analysis and reporting. As a result of observations from recent studies with welds removed from retired steam generators of the Palisades Nuclear Plant, the Nuclear Regulatory Commission (NRC) requested ORNL and other NRC contractors to prepare a letter report on thermal aging determination of copper content for welds fabricated with copper-coated weld wire. Analysis of all available data concluded that no trends indicate significant thermal embrittlement, although potential mechanisms for thermal embrittlement are possible. Regarding chemical composition, methods for determination of copper content and specific recommendations regarding coil-weighted versus weld-weighted averaging were described within a statistical context. Specimens of two Russian weld metals irradiated at the University of Michigan FNR were returned to ORNL. Most of the correlation monitor material was placed into storage racks in the new long-term storage facility at ORNL. Additionally, pieces of HSST plate 03 were distributed to participants in the ASTM cross-comparison exercise on subsize specimen testing technology. The final design of the irradiation facility and specimen baskets for University of California, Santa Barbara, irradiations was conceptually completed. The resulting design should permit the irradiation of all test specimens to within 5°C of their desired temperature. Detailing of all parts was begun.

Contents

Contents (continued)

Figures

Contents (continued)

Figures

Contents (continued)

Figures

Tables

Contents (continued)

Tables

Acknowledgments

The authors thank Julia Bishop for her contributions in the preparation of the draft manuscript for this report, M. R. Upton for the final manuscript preparation, K. Spence for editing and quality assurance review. The authors also gratefully acknowledge the continuing technical and financial contributions of the Nuclear Regulatory Commission to the Heavy-Section Steel Irradiation Program.

Preface

The primary goal of the Heavy-Section Steel Irradiation (HSSI) Program is to provide a thorough, quantitative assessment of the effects of neutron irradiation on the material behavior and, in particular, the fracture toughness properties of typical pressure-vessel steels as they relate to light-water reactor pressure vessel (RPV) integrity. The program includes studies of the effects of irradiation on the degradation of mechanical and fracture properties of vessel materials augmented by enhanced examinations and modeling of the accompanying microstructural changes. Effects of specimen size; material chemistry; product form and microstructure; irradiation fluence, flux, temperature, and spectrum; and postirradiation annealing are being examined on a wide range of fracture properties. Results from the HSSI studies will be incorporated into codes and standards directly applicable to resolving major regulatory issues which involve RPV irradiation embrittlement such as pressurized-thermal shock, operating pressure-temperature limits, low-temperature overpressurization, and the specialized problems associated with low upper-shelf welds.

This HSSI Program progress report covers work performed from October 1994 to March 1995. The work performed by Oak Ridge National Laboratory (ORNL) is managed by the Metals and Ceramics (M&C) Division of ORNL. Major tasks at ORNL are carried out by the M&C, Computing Physics and Engineering, and Engineering Technology Divisions.

Previous HSSI Progress Reports in this series are:

NUREG/CR-5591, Vol. 1, No. 1
(ORNL/TM-11568/V1&N1)
NUREG/CR-5591, Vol. 1, No. 2
(ORNL/TM-11568/V1&N2)
NUREG/CR-5591, Vol. 2, No. 1
(ORNL/TM-11568/V2&N1)
NUREG/CR-5591, Vol. 2, No. 2
(ORNL/TM-11568/V2&N2)
NUREG/CR-5591, Vol. 3
(ORNL/TM-11568/V3)
NUREG/CR-5591, Vol. 4, No. 1
(ORNL/TM-11568/V4&N1)
NUREG/CR-5591, Vol. 4, No. 2
(ORNL/TM-11568/V4&N2)
NUREG/CR-5591, Vol. 5, No. 1
(ORNL/TM-11568/V5&N1)
NUREG/CR-5591, Vol. 5, No. 2
(ORNL/TM-11568/V5&N2)

Some of the series of irradiation studies conducted within the HSSI Program were begun under the Heavy-Section Steel Technology (HSST) Program prior to the separation of the two programs in 1989. Previous HSST Program progress reports contain much information on the irradiation assessments being continued by the HSSI Program as well as earlier related studies. The HSST Program progress reports issued before formation of the HSSI Program are also tabulated here as a convenience to the reader.

ORNL-4176
ORNL-4315
ORNL-4377
ORNL-4463
ORNL-4512
ORNL-4590
ORNL-4653
ORNL-4681
ORNL-4764

ORNL-4816
ORNL-4855
ORNL-4918
ORNL-4971
ORNL/TM-4655 (Vol. II)
ORNL/TM-4729 (Vol. II)
ORNL/TM-4805.(Vol. II)
ORNL/TM-4914 (Vol. II)
ORNL/TM-5021 (Vol. II)
ORNL/TM-5170
ORNL/NUREG/TM-3
ORNL/NUREG/TM-28
ORNL/NUREG/TM-49
ORNL/NUREG/TM-64
ORNL/NUREG/TM-94
ORNL/NUREG/TM-120
ORNL/NUREG/TM-147
ORNL/NUREG/TM-166
ORNL/NUREG/TM-194
ORNL/NUREG/TM-209
ORNL/NUREG/TM-239
NUREG/CR-0476 (ORNL/NUREG/TM-275)
NUREG/CR-0656 (ORNL/NUREG/TM-298)
NUREG/CR-0818 (ORNL/NUREG/TM-324)
NUREG/CR-0980 (ORNL/NUREG/TM-347)
NUREG/CR-1197 (ORNL/NUREG/TM-370)
NUREG/CR-1305 (ORNL/NUREG/TM-380)
NUREG/CR-1477 (ORNL/NUREG/TM-393)
NUREG/CR-1627 (ORNL/NUREG/TM-401)
NUREG/CR-1806 (ORNL/NUREG/TM-419)
NUREG/CR-1941 (ORNL/NUREG/TM-437)
NUREG/CR-2141, Vol. 1 (ORNL/TM-7822)
NUREG/CR-2141, Vol. 2 (ORNL/TM-7955)
NUREG/CR-2141, Vol. 3 (ORNL/TM-8145)
NUREG/CR-2141, Vol. 4 (ORNL/TM-8252)
NUREG/CR-2751, Vol. 1 (ORNL/TM-8369/V1)
NUREG/CR-2751, Vol. 2 (ORNL/TM-8369/V2)
NUREG/CR-2751, Vol. 3 (ORNL/TM-8369/V3)
NUREG/CR-2751, Vol. 4 (ORNL/TM-8369/V4)
NUREG/CR-3334, Vol. 1 (ORNL/TM-8787/V1)
NUREG/CR-3334, Vol. 2 (ORNL/TM-8787/V2)
NUREG/CR-3334, Vol. 3 (ORNL/TM-8787/V3)
NUREG/CR-3744, Vol. 1 (ORNL/TM-9154/V1)
NUREG/CR-3744, Vol. 2 (ORNL/TM-9154/V2)
NUREG/CR-4219, Vol. 1 (ORNL/TM-9593/V1)
NUREG/CR-4219, Vol. 2 (ORNL/TM-9593/V2)
NUREG/CR-4219, Vol. 3, No. 1 (ORNL/TM-9593/V3&N1)
NUREG/CR-4219, Vol. 3, No. 2 (ORNL/TM-9593/V3&N2)
NUREG/CR-4219, Vol. 4, No. 1 (ORNL/TM-9593/V4&N1)
NUREG/CR-4219, Vol. 4, No. 2 (ORNL/TM-9593/V4&N2)
NUREG/CR-4219, Vol. 5, No. 1 (ORNL/TM-9593/V5&N1)
NUREG/CR-4219, Vol. 5, No. 2 (ORNL/TM-9593/V5&N2)

Summary

1. Program Management

The Heavy-Section Steel Irradiation (HSSI) Program is arranged into 14 tasks: (1) program management, (2) fracture toughness curve shift in high-copper weldments (Series 5 and 6), (3) K_{Ic} and K_{Ia} curve shifts in low upper-shelf (LUS) welds (Series 8), (4) irradiation effects in a commercial LUS weld (Series 10), (5) irradiation effects on weld heat-affected zone (HAZ) and plate materials (Series 11), (6) annealing effects in LUS welds (Series 9), (7) microstructural and microfracture analysis of irradiation effects, (8) in-service irradiated and aged material evaluations, (9) Japan Power Development Reactor (JPDR) steel examination, (10) fracture toughness curve shift method, (11) special technical assistance, (12) technical assistance for Joint Coordinating Committee on Civilian Nuclear Reactor Safety (JCCCNRS) Working Groups 3 and 12, (13) correlation monitor materials, and (14) test reactor coordination. Report chapters correspond to the tasks. The work is performed by the Oak Ridge National Laboratory (ORNL). During the report period, four technical papers, one letter report, and five foreign trip reports were published. In addition, 15 technical presentations were made.

2. Fracture Toughness Shift in High-Copper Weldments (Series 5 and 6)

The objective of this task is to develop data addressing the current method of shifting the American Society of Mechanical Engineers (ASME) fracture toughness (K_{Ic}, K_{Ia}, and K_{IR}) curves to account for irradiation embrittlement in high-copper welds. The specific activities to be performed in this task are the: (1) continuation of Phase 2 of the Fifth Irradiation Series; and (2) completion of the Sixth Irradiation Series, including testing nine irradiated Italian crack-arrest specimens. The test results of the Italian crack-arrest specimens are being analyzed, and full details will be published in a NUREG report currently in preparation. The crack-mouth opening displacement (CMOD) was measured at a distance greater than that prescribed in the American Society for Testing and Materials (ASTM) Test for Determining Plane-Strain Crack-Arrest Fracture Toughness, K_{Ia}, of Ferritic Steels (E 1221-88). A method for adjusting the CMOD to account for this has been developed and is presented. The correction was ~4% for small specimens and ~2% for the larger ones. As part of this task, irradiation of HSSI weld 73W to a high fluence [5×10^{19} neutrons/cm^2 (> 1 MeV)] will be performed to determine whether the K_{Jc} curve shape change observed in the Fifth HSSI Series is exacerbated. The design and fabrication of the temperature and dosimetry verification capsules are performed under this task, but for purposes of continuity, their progress will be reported under Task 6, where the design of the new irradiation facilities and capsules is performed.

3. Fracture Toughness Curve Shift in Low Upper-Shelf Welds (Series 8)

This task examines the fracture toughness curve shifts and changes in shape for irradiated welds with low Charpy V-notch (CVN) upper-shelf energy (USE). This task was specifically designed to address questions raised by the Advisory Committee for Reactor Safeguards concerning the shape of the K_{Ic} curve for irradiated welds with a low USE. In particular, it will clarify whether the high concentration of inclusions in low-USE welds results in a transition relationship and behavior significantly different from high-USE welds. The information developed under this task will augment information obtained from other HSSI tasks performed on two high-USE weldments under the Fifth and Sixth Irradiation Series and on a commercial, low USE under the Tenth Irradiation Series. The results will provide an expanded basis for accounting for irradiation-induced embrittlement in reactor pressure vessel (RPV) materials.

Three low-USE welds have been ordered from ABB-Combustion Engineering (ABB-CE), Chattanooga, Tennessee and two of them have been delivered to ORNL. ABB-CE fabricated the welds for the Fifth and Sixth Series.

4. Irradiation Effects in a Commercial Low Upper-Shelf Weld (Series 10)

The objective of this task is to evaluate the chemical, mechanical, and fracture properties of the WF-70 weld metal at the beltline and nozzle course locations in the Midland Unit 1 reactor vessel. CVN transition temperature curves of unirradiated weld metal were generated at 19 positions throughout the beltline weld and at 6 positions throughout the nozzle course weld. The transition temperature ranged from –20 to 37°C for the beltline weld and from –8 to 18°C for the nozzle course weld. The USE was similar for both welds at 88 J (65.3 ft-lb). Drop weight (DWT) nil-ductility transition (NDT) tests confirmed the similarity of unirradiated transition temperature, nominally at –55°C (–67°F) for both welds.

CVN specimens of beltline and nozzle course weld material were irradiated in separate capsules (scoping capsules 10.01 and 10.02) to 0.5×10^{19} neutrons/cm^2 (< 1 MeV) and to 1×10^{19} neutrons/cm^2 (< 1 MeV) [capsule 10.05]. These tests suggest that the kinetics of damage development are sensitive to copper content, with the higher copper content material showing larger shifts in transition temperature and greater decreases in USE than the lower copper material.

Data from fracture mechanics testing were used to benchmark ASME methods currently in use. For the beltline weld, the average initial RT_{NDT} from 19 individual CVN transition temperature determinations was 8°C (46°F). The transition temperature shift at the 41-J (30-ft-lb) level and at 1×10^{19} neutrons/cm^2 was 104°C (187°F). This information was used to establish the positions on the abscissa (temperature axis) for the lower-bound K_{Ic} curve. The two ASME lower-bound K_{Ic} curves are positioned very conservatively. The 5% lower-bound curve on the master curve, offset by only a 10°C margin, bounds the experimental data more accurately.

It may be possible to use Charpy specimens to generate data equivalent to that obtained from much larger fracture mechanics specimens. Crack-arrest events often seen in autographic load-time traces during the standard CVN impact tests may be related to K_{Ia} transition curves. For the WF-70 beltline weld metal, the shift in K_{Ia} transition temperature derived from Charpy tests appears to be only one-half of the 41-J transition temperature shift. Large specimens are available to check this result.

Another possibility currently being explored is to use precracked specimens and then test them as fracture mechanics three-point bend bars. A proposed ASTM test practice currently under development was used to obtain T_o reference temperatures from both beltline and nozzle course weld metals before and after irradiation at 1×10^{19} neutrons/cm^2. A few of the specimens tested suffered from loss of constraint, and the K_{Jc} values were elevated above an acceptable limit; a data-censoring technique was applied in the analysis of these data. The results from beltline weld metal were compatible with the results from larger fracture mechanics specimens. However, the lower initial toughness of the nozzle course material was not confirmed by the Charpy specimens.

Capsule 10.06 was shipped to ORNL from the Ford Nuclear Reactor (FNR) as planned. Disassembly has been delayed pending approval to proceed with that particular project task (Task 4.2). A preliminary report on the exposure parameters for capsule 10.05 [1×10^{19} neutrons/cm^2 (< 1 MeV)] has been prepared and is undergoing internal peer review.

5. Irradiation Effects On Weld Heat-Affected Zone and Plate Materials (Series 11)

The purpose of this task is to examine the effects of neutron irradiation on the fracture toughness (ductile and brittle) of the HAZ of welds of A 302 grade B (A302B) plate materials typical of those used in fabricating older RPVs. The initial plate material of emphasis will be A302B steel, not the A302B modified with nickel additions. For the HAZ portion of the program, the intent is to examine HAZ material in the A302B (i.e., with low nickel content), and in A302B (modified) or A533B-1 (i.e., with medium nickel content). Two specific plates were identified as being applicable to this task. One plate is A302B and the other is A302B (modified). The A302B

plate will be prepared for welding, while the A302B (modified) plate already contains a commercially produced weld. The materials have been requested from Yankee Atomic Electric Company (YAEC) for use in this irradiation task, and arrangements are being made with YAEC for procurement of the plates mentioned above.

6. Annealing Effects in Low Upper-Shelf Welds (Series 9)

The purpose of the Ninth Irradiation Series is to evaluate the correlation between fracture toughness and CVN impact energy during irradiation, annealing, and reirradiation (IAR).

Effects of annealing on the CVN impact energy specimens from the low-USE welds from the Midland beltline and nozzle course welds, as well as HSST plate 02 and HSSI weld 73W, were examined as was the effect of annealing on the initiation fracture toughness of annealed material from Midland beltline weld and HSST plate 02. The results from capsule 10.05 specimens of weld 73W confirm those previously obtained on the so-called undersize specimens that were irradiated in the Fifth Irradiation Series, namely that the recovery due to annealing at 343°C (650°F) for 1 week is insignificant.

The fabrication of major components for the IAR facility for two positions on the east side of the FNR at the University of Michigan has begun. Fabrication of two reusable capsules (one for temperature verification and the other for dosimetry verification), as well as two capsules for IAR studies, is also under way. The design of a reusable capsule capable of reirradiating previously irradiated and annealed CVN and 1T C(T) specimens is also progressing. The data acquisition and control instrumentation for the first two IAR facilities is essentially complete and awaiting completion of the IAR facilities and temperature test capsule for checkout and control algorithm development.

7. Microstructural and Microfracture Analysis of Irradiation Effects

The overall long-term goal of this task is to develop a physically based model which can be used to predict irradiation-induced embrittlement in reactor vessel steels over the full range of their service conditions. The model should be tethered soundly on the microstructural level by results from advanced microstructural analysis techniques and constrained at the macroscopic level to produce predictions consistent with the large array of macroscopic embrittlement measurements that are available. During this reporting period, characterization of long-term (~ 100,000 h) thermally aged and neutron-irradiated surveillance materials by atom-probe field-ion microscopy indicated that thermal aging did not result in any copper clustering or compositional changes in the ferrite matrix. A comparison with the as-fabricated welds verified that copper precipitation during the postweld heat treatment had reduced the matrix copper content below the nominal bulk value. Analysis of ion-irradiated model alloys has demonstrated the role of point defect clusters in hardening. A preliminary microstructure/ hardening correlation has been obtained. A significant body of French pressurized-water reactor surveillance data has been obtained and formatted for comparison with U.S. data and for use in calibrating kinetic embrittlement models.

8. In-Service Irradiated and Aged Material Evaluations

The objective of this task is to provide a direct assessment of actual material properties in irradiated components of nuclear reactors, including the effects of irradiation and aging. Four activities are currently in progress: (1) establishing a machining capability for contaminated or activated materials by completing procurement and installation of a computer-based milling machine in a hot cell, (2) machining and testing specimens from cladding materials removed from the Gundremmingen reactor to establish their fracture properties, (3) preparing an interpretive report on the effects of neutron irradiation on cladding, and (4) continuing the evaluation of long-term aging at low temperatures of austenitic structural stainless steel weld metal.

Drawings were made for hot cell installation of the computer numerically controlled machining center and for installing a new saw for use inside the hot cell.

Tensile, CVN, and fracture toughness testing of three-wire stainless steel cladding, thermally aged for 20,000 h at 288 or at 343°C, was completed and a draft report was prepared. The test results show that the effects of thermal aging at either temperature were very small and similar to those reported earlier for 1605 h aging at 288°C. Tensile tests of type 308 stainless steel weld metal, aged at 343°C for 50,000 h, showed that aging has little effect on the tensile properties.

9. Evaluation of Steel from the JPDR Pressure Vessel

There is a need to validate the results of irradiation effects research by the examination of material taken directly from the wall of a pressure vessel which has been irradiated during normal service. This task has been included with the HSSI Program to provide just such an evaluation on material from the wall of the pressure vessel from the JPDR. During this reporting period, detailed plans were implemented and work was virtually concluded to evaluate the existing neutron dosimetry and transport calculations which have been performed for the JPDR by the Japanese as well as to perform similar transport calculations at ORNL. The ORNL transport calculations included the concrete in the biological shield as well as the pressure vessel. This allowed participation in the International Atomic Energy Agency exercise on concrete activation for decommissioning, as well as the original program aims to determine flux and fluence levels within the vessel itself.

10. Fracture Toughness Curve Shift Method

The purpose of this task is to examine the technical basis for the currently accepted methods for shifting fracture toughness curves to account for irradiation damage, and to work through national codes and standards bodies to revise those methods, if a change is warranted. Specific activities under this task include: (1) collection and statistical analysis of pertinent fracture toughness data to assess the shift and potential change in shape of the fracture toughness curves due to neutron irradiation, thermal aging, or both; (2) evaluation of methods for indexing fracture toughness curves to values that can be deduced from material surveillance programs required under the *Code of Federal Regulations* (10CFR50), Appendix H; (3) participation in the pertinent ASME Section XI, ASTM E-8, and ASTM E-10 committees; (4) interaction with other researchers in the national and international technical community addressing similar problems; and (5) frequent interactions and detailed technical meetings with the Nuclear Regulatory Commission (NRC) staff.

Data from all the relevant HSSI Programs were acquired and stored in a data base and evaluated. A method employing Weibull statistics was applied to analyze fracture toughness properties of unirradiated and irradiated pressure vessel steels. Application of the concept of a master curve for irradiated materials was examined and used to measure shifts of fracture toughness transition curves. It was shown that the maximum likelihood approach gave good estimations of the reference temperature, T_o, determined by rank method and could be used for analyzing data sets where application of the rank method did not prove to be feasible.

It was shown that, on average, the fracture toughness shifts generally exceeded the Charpy 41-J shifts; a linear least-squares fit to the data set yielded a slope of 1.15. The observed dissimilarity was analyzed by taking into account differences in effects of irradiation on Charpy impact and fracture toughness properties. Based on these comparisons, a procedure to adjust Charpy 41-J shifts for achieving a more reliable correlation with the fracture toughness shifts was evaluated. All these procedures are still under evaluation and will be evaluated with the larger data base which is being assembled.

11. Special Technical Assistance

This task has been included within the HSSI Program to provide a vehicle in which to conduct and monitor short-term, high-priority subtasks and provide technical expertise and assistance in the review of national codes and standards that may be referenced in NRC regulations or guides related to nuclear reactor components. This

task currently addresses two major areas: (1) providing technical expertise and assistance in the review of national codes and standards and (2) experimental evaluations of test specimens and practices and material properties. The following activities occurred during this reporting period.

SRI has completed initial testing of notched round bar specimens fabricated from weld 72W material. A final report has been written describing the test methods and results. The report will be issued as a NUREG (ORNL/TM) report. Round tensile bars, 6 mm in diameter, were precracked in rotating 4-point bending. This technique produced uniform annular precracks with very low eccentricity. The specimens were tested over a range of temperatures from –150 to 50°C. The area under the load-displacement curve was used to calculate the J-integral. The crack length was measured from the fracture surface after completion of the test. The results were compared to tests conducted at ORNL of 1T compact specimens from an essentially identical weld. The notched round bar results agree well with the 1T compact data in the middle of the transition regime, but tend to show higher toughness than the 1T specimens at lower test temperatures. Suggested reasons for the difference are: (1) possible inaccuracies in the J-integral formula, (2) differences in constraint between the two specimen types, (3) statistical size effects, and (4) possible differences between the two welds.

A draft report describing the testing of subsize Charpy specimens has been written and is undergoing internal review. A new approach to normalizing data from subsize specimens was developed. This method gives excellent agreement with the data from full-size specimens for materials that have USE levels less than about 200 J. Ten material variants and five designs of subsize specimens were chosen for the study. The normalization procedure of the data from subsize specimens involved two steps: a transformation of the energy values, followed by a temperature shift. The energy was divided into brittle and ductile components, based on the fracture surface appearance or the amount of rapid load drop from the voltage-time trace from the instrumented tup. The low-energy cleavage fracture was scaled by the ratio of the notched cross-sectional area of the full-size to the subsize specimen. The high-energy ductile fracture portion was scaled by an empirically determined value for the ratio of the USE of full-size to subsize specimens, unique for each type of subsize specimen. The scaled energy value was then given a new temperature value by adding an empirically determined correction factor. This normalization process gives excellent agreement between the corrected subsize data and the data from the full-size specimens.

All of the reconstituted Charpy specimens have been tested for the ASTM round robin. The results have been tabulated and transmitted to ASTM for their analysis and reporting.

As a result of observations from recent studies with welds removed from retired steam generators of the Palisades Nuclear Plant, the NRC requested ORNL and other NRC contractors to prepare a letter report considering two topics: (1) preliminary review of thermal aging of RPV steels under nominal reactor operating conditions, and (2) considerations in determination of copper content for welds fabricated with copper-coated weld wire. The letter report included discussions on (1) data from the literature regarding relatively low-temperature thermal embrittlement of RPV steels, (2) relevant data from the power reactor-embrittlement data base (PR-EDB), (3) potential mechanisms of thermal embrittlement in low-alloy, and (4) the mechanical property and chemical composition data reported by Consumers Power Company for the steam generator welds and the data base for welds fabricated with weld wire W5214. Most of the data from the literature suggest no substantial embrittlement for typical RPV steels in the temperature range of interest for up to 100,000 h. However, the potential for thermal embrittlement for times up to 30 to 40 years cannot be dismissed based on the data available. Furthermore, the known synergistic effects of copper and nickel, as well as nickel and phosphorus, do not allow us to assume that the observations from the literature are necessarily directly indicative of the entire range of materials of interest in U.S. RPVs. Although the review of the PR-EDB showed the peak in the distribution of number of data points versus exposure time is at 2 years, there are over 100 data points available with over 6 years exposure. Analysis of those data concluded that no trends are evident in the PR-EDB data to indicate thermal embrittlement. The review of potential mechanisms for thermal embrittlement concluded that such aging effects are possible under the conditions evaluated but may be rare and dependent on many factors. It was felt that independent aging effects should not be simply added to irradiation-induced embrittlement. Based on statistical analyses of the available DWT and Charpy impact data from the steam generator weld W5214 (SG-A), the weld transition temperature is not so far from the average of other estimates for the same weld wire that we judge the SG-A weld estimate to be significantly different. Regarding chemical composition of the SG-A weld, the evaluation focused

on methods for determination of copper content and makes specific recommendations regarding coil-weighted versus weld-weighted averaging, all of which are discussed within a statistical context. It was recommended that a single average value be obtained from the new copper measurements on the SG-A weld, which is noted to provide a bimodal distribution of copper.

12. Technical Assistance for JCCCNRS Working Groups 3 and 12

The purpose of this task is to provide technical support for the efforts of the U.S.-Russian JCCCNRS Working Group 3 on radiation embrittlement and Working Group 12 on aging. Specific activities under this task are: (1) supply of materials and preparation of test specimens for collaborative IAR studies to be conducted in Russia; (2) capsule preparation and initiation of irradiation of Russian specimens within the United States; (3) preparation for, and participation in, working Groups 3 and 12 meetings; and (4) sponsoring of the assignment at ORNL of a scientist from the Russian National Research Center, Kurchatov Institute.

Specimens of two Russian weld metals irradiated in HSSI capsule 10.06 at the University of Michigan FNR have been returned to ORNL. Testing of the Russian materials is anticipated to be completed prior to the end of 1995.

The sabbatical of Dr. Mikhail A. Sokolov at ORNL continued. The results of his research are presented within the particular technical tasks of HSSI semiannual progress reports and published technical reports and papers.

13. Correlation Monitor Materials

This is a task that has been established with the explicit purpose of ensuring the continued availability of the pedigreed and extremely well-characterized material now required for inclusion in all additional and future surveillance capsules in commercial light-water reactors. Having recognized that the only remaining materials qualified for use as a correlation monitor in reactor surveillance capsules are the pieces remaining from the early HSST plates 01, 02, and 03, this task will provide for cataloging, archiving, and distributing the material on behalf of the NRC. During this reporting period, concrete was poured, pallet storage racks were installed, and most of the material was placed into the storage racks. Additionally, pieces of HSST plate 03 were distributed to participants in the ASTM cross-comparison exercise on subsize specimen testing technology.

14. Test Reactor Irradiation Coordination

The purpose of this task is to provide the support required to supply and coordinate irradiation services needed by NRC contractors other than ORNL. These services include the design and assembly of irradiation capsules as well as arranging for their exposure, disassembly, and return of specimens. Currently, the University of California, Santa Barbara, is the only other NRC contractor for whom irradiations are to be conducted. During this reporting period, the final design of the irradiation facility and specimen baskets was determined through an iterative process involving the designers and thermal analysts. The resulting design should permit the irradiation of all test specimens to within 5°C of their desired temperature. Detailing of all parts is ongoing and should be completed during the next reporting period. Procurement of the facility will also be initiated during the next reporting period.

Heavy-Section Steel Irradiation Program Semiannual Progress Report for October 1994 through March 1995*,†

W. R. Corwin

1. Program Management

The Heavy-Section Steel Irradiation (HSSI) Program, a major safety program sponsored by the Nuclear Regulatory Commission (NRC) at Oak Ridge National Laboratory (ORNL), is an engineering research activity devoted to providing a thorough, quantitative assessment of the effects of neutron irradiation on the material behavior, particularly the fracture toughness properties, of typical pressure-vessel steels as they relate to light-water reactor pressure vessel (RPV) integrity. The program centers on experimental assessments of irradiation-induced embrittlement [including the completion of certain irradiation studies previously conducted by the Heavy-Section Steel Technology (HSST) Program] augmented by detailed examinations and modeling of the accompanying microstructural changes. Effects of specimen size; material chemistry; product form and microstructure; irradiation fluence, flux, temperature, and spectrum; and postirradiation annealing are being examined on a wide range of fracture properties. Fracture toughness (K_{Ic} and J_{Ic}), crack-arrest toughness (K_{Ia}), ductile tearing resistance (dJ/da), Charpy V-notch (CVN) impact energy, drop-weight (DWT) nil-ductility transition (NDT), and tensile properties are included. Models based on observations of radiation-induced microstructural changes using the atom-probe field-ion microscope (APFIM) and the high-resolution transmission electron microscope (TEM) are being developed to provide a firm basis for extrapolating the measured changes in fracture properties to wide ranges of irradiation conditions. The principal materials examined within the HSSI Program are high-copper welds because their postirradiation properties frequently limit the continued safe operation of commercial RPVs. In addition, a limited effort will focus on stainless steel weld-overlay cladding typical of that used on the inner surfaces of RPVs because its postirradiation fracture properties have the potential for strongly affecting the extension of small surface flaws during overcooling transients.

Results from the HSSI studies will be integrated to aid in resolving major regulatory issues facing the Nuclear Regulatory Commission (NRC). Those issues involve RPV irradiation embrittlement such as pressurized-thermal shock, operating pressure-temperature limits, low-temperature overpressurization, and the specialized problems associated with low upper-shelf (LUS) welds. Together, the results of these studies also provide guidance and bases for evaluating the overall aging behavior of light-water RPVs.

The program is coordinated with those of other government agencies and the manufacturing and utility sectors of the nuclear power industry in the United States and abroad. The overall objective is the quantification of irradiation effects for safety assessments of regulatory agencies, professional code-writing bodies, and the nuclear power industry.

The program is broken down into 1 task responsible for overall program management and 13 technical tasks: (1) program management, (2) fracture toughness curve shift in high-copper weldments (Series 5 and 6), (3) K_{Ic} and K_{Ia} curve shifts in LUS welds (Series 8), (4) irradiation effects in a commercial LUS weld (Series 10), (5) irradiation effects on weld heat-affected zone (HAZ) and plate materials (Series 11), (6) annealing effects in LUS welds (Series 9), (7) microstructural and microfracture analysis of irradiation effects, (8) in-service irradiated and aged material evaluations, (9) Japan Power Development Reactor (JPDR) steel examination, (10) fracture

*Research sponsored by the Office of Nuclear Regulatory Research, U.S. Nuclear Regulatory Commission, under Interagency Agreement DOE 1886-8109-8L with the U.S. Department of Energy under contract DE-AC05-84OR21400 with Lockheed Martin Energy Systems.

toughness curve shift method, (11) special technical assistance, (12) technical assistance for Joint Coordinating Committee on Civilian Nuclear Reactor Safety (JCCCNRS) Working Groups 3 and 12, (13) correlation monitor materials, and (14) test reactor coordination.

During this period, eight program briefings, reviews, or presentations were made by the HSSI staff during program reviews and visits with NRC staff or others. Four technical papers,[1-4] one letter report,[5] and five foreign trip reports[6-10] were published. In addition, 15 technical presentations were made.[11-25]

References

1. D. E. McCabe, R. K. Nanstad, S. K. Iskander, and R. L. Swain, Martin Marietta Energy Systems, Inc., Oak Ridge Natl. Lab., *Unirradiated Material Properties of Midland Weld WF-70*, USNRC Report, NUREG/CR-6249 (ORNL/TM-12777), October 1994.*

2. R. E. Stoller, Martin Marietta Energy Systems, Inc., Oak Ridge Natl. Lab., *A Comparison of the Relative Importance of Copper Precipitates and Point Defect Clusters in Reactor Pressure Vessel Embrittlement*, USNRC Report, NUREG/CR-6231 (ORNL-6811), December 1994.*

3. W. R. Corwin, Martin Marietta Energy Systems, Inc., Oak Ridge Natl. Lab., *Semiannual Progress Report for April 1993 - September 1993,* USNRC Report, NUREG/CR-5591, Vol. 4, No. 2, ORNL/TM-11568/V4&N2, October 1994.*

4. S. K. Iskander, M. A. Sokolov, and R. K. Nanstad, "Some Aspects of the Role of Annealing in Plant Life Extension," *Trans. Am. Nucl. Soc.* **71**, 191-92 (1994).†

5. R. K. Nanstad, D. J. Alexander, W. R. Corwin, E. D. Eason, G. R. Odette, R. E. Stoller, and J. A. Wang, Martin Marietta Energy Systems, Inc., Oak Ridge Natl. Lab., *Preliminary Review of Data Regarding Chemical Composition and Thermal Embrittlement of Reactor Vessel Steels*, Letter Report, ORNL/NRC/LTR-95/1, January 1995.

6. S. K. Iskander, *Report of Foreign Travel to Italy*, ORNL/FTR-5160, October 25, 1994.*

7. R. K. Nanstad, F. B. Kam, and G. R. Odette, *Report of Foreign Travel to Ukraine and Russia*, ORNL/FTR-5139, November 10, 1994.*

8. R. K. Nanstad and C. J. Fairbanks, *Report of Foreign Travel to United Kingdom*, ORNL/FTR-5213, November 29, 1994.*

9. S. K. Iskander and A. Taboada, *Report of Foreign Travel to Japan*, ORNL/FTR-5173, December 20, 994.*

10. B. L. Broadhead, *Report of Foreign Travel to Austria*, ORNL/FTR-5266, December 22, 1994.*

11. W. R. Corwin and W. E. Pennell, "Reactor Pressure Vessel Structural Integrity Research," presented at the 22nd Water Reactor Safety Meeting, Bethesda, Maryland, October 24, 1994.

12. S. K. Iskander, M. A. Sokolov, R. K. Nanstad, and A. Taboada, "Some Aspects of Annealing of Nuclear Reactor Pressure Vessels as a Lifetime Management Resource," presented at International Atomic Energy Agency International Working Group on Life Management of Nuclear Power Plants, Specialists Meeting on Technology for Lifetime Management of Nuclear Power Plants, Tokyo, Japan, November 15-17, 1994.

*Available for purchase from National Technical Information Service, Springfield, VA 22161.

†Available in public technical libraries.

13. S. K. Iskander, M. A. Sokolov, and R. K. Nanstad, "Some Aspects of the Role of Annealing in Plant Life Extension," presented at the American Nuclear Society Winter Meeting, Washington, D.C., November 13-17, 1994.

14. R. E. Stoller, "Molecular Dynamics Simulations of High Energy Cascades in Iron," presented at the 1994 Fall Meeting of the Materials Research Society, Boston, November 28 - December 2, 1994.

15. P. M. Rice and R. E. Stoller, "Correlation of Mechanical Property Changes with Microstructural Changes in Ion-irradiated Model Pressure Vessel Steels," presented at the 1994 Fall Meeting of the Materials Research Society, Boston, November 28 - December 2, 1994.

16. D. E. Alexander, L. E. Rehn, K. Farrell, and R. E. Stoller, Gamma Ray-Induced Embrittement of Pressure Vessel Alloys," presented at the 1994 Fall Meeting of the Materials Research Society, Boston, November 28 - December 2, 1994.

17. W. R. Corwin, "Pressure Vessel Materials Research at ORNL," presented at the NUPEC - DOE Meeting, Albuquerque, New Mexico, February 2, 1995.

18. D. J. Alexander, K. B. Alexander, M. K. Miller, and R. K. Nanstad, "The Effects of Aging at 343°C to 50,000 hours on the Mechanical Properties of Type 308 Stainless Steel Weld Metal," presented at TMS-AIME Symposium on Microstructure and Mechanical Properties of Aging Materials, Las Vegas, Nevada, February 12-16, 1995.

19. D. J. Alexander, J. M. Vitek, and S. A. David, "The Effects of Aging at 400 to 500°C on the Microstructure and Mechanical Properties of Type 308 Stainless Steel Weldments," presented at TMS-AIME Symposium on Microstructure and Mechanical Properties of Aging Materials, Las Vegas, Nevada, February 12-16, 1995.

20. D. E. McCabe, "Irradiation of Low Upper-Shelf Weld Metal WF-70 from the Midland Reactor," presented at B&W Owners Group/ORNL/NRC Meeting, Knoxville, Tennessee, March 23, 1995.

21. M. A. Sokolov, S. K. Iskander, and R. K. Nanstad, "HSSI Program Includes Annealing and Reirradiation of High-Copper, Low Upper-Shelf Welds," presented at B&W Owners Group/ORNL/NRC Meeting, Knoxville, Tennessee, March 23, 1995.

22. R. E. Stoller, "Atom Probe Analysis of Thermally Aged Materials," presented at B&W Owners Group/ORNL/NRC Meeting, Knoxville, Tennessee, March 23, 1995.

23. W. R. Corwin, "Overview of the HSSI Program," presented at B&W Owners Group/ORNL/NRC Meeting, Knoxville, Tennessee, March 23, 1995.

24. R. K. Nanstad, S. K. Iskander, and M. A. Sokolov, "HSSI Thermal Annealing Task Involves Short- and Long-Term Studies, Including Reembrittlement," presented at B&W Owners Group/ORNL/NRC Meeting, Knoxville, Tennessee, March 23, 1995.

25. D. E. McCabe, "Overview of the Practice, Objectives, and Mechanics of the Approach," presented at the meeting of the ASTM Working Group on Ductile-to-Brittle Test Practice, Rockville, Maryland, March 26-28, 1995.

2. Fracture Toughness Shifts In High-Copper Weldments (Series 5 And 6)

S. K. Iskander

2.1 Introduction

The objective of this task is to develop data addressing the current method of shifting the American Society of Mechanical Engineers (ASME) fracture toughness (K_{Ic}, K_{Ia}, and K_{IR}) curves to account for irradiation embrittlement in high-copper welds. The specific activities to be performed in this task are the: (1) continuation of Phase 2 of the Fifth Irradiation Series, and (2) completion of the Sixth Irradiation Series, including testing nine irradiated Italian crack-arrest specimens. The test results of the Italian crack-arrest specimens are being analyzed, and full details will be published in a NUREG report currently in preparation. The crack-mouth opening displacement (CMOD) was measured at a distance greater than that prescribed in the American Society for Testing and Materials (ASTM) "Test for Determining Plane-Strain Crack-Arrest Fracture Toughness, K_{Ia}, of Ferritic Steels" (E 1221-88). A method for adjusting the CMOD to account for this has been developed and is presented. The correction was ~4% for small specimens and ~2% for the larger ones. As part of this task, irradiation of HSSI weld 73W to a high fluence [5×10^{19} neutrons/cm^2 (> 1 MeV)] will be performed to determine whether the K_{Jc} curve shape change observed in the Fifth HSSI Series is exacerbated. The design and fabrication of the temperature and dosimetry verification capsules are performed under this task, but for purposes of continuity, their progress will be reported under Task 6, where the design of the new irradiation facilities and capsules is performed.

The Italian nuclear regulatory authorities, Agenzia Nazionale per la Protezione dell'Ambiente (ANPA), started an extensive research program some time ago to characterize an ASTM A 508 class 3 forging produced in Italy.[1] The research program encompassed both unirradiated and irradiated mechanical property data from tensile, Charpy impact (both standard and precracked), compact tensile, and crack-arrest specimens. Several institutions are involved in the irradiation and testing of these specimens: ANPA CRE Casaccia Laboratories, Battelle Columbus Laboratories (BCL), and two laboratories of the French Commissariat a l'Energie Atomique. ANPA originally planned to test the irradiated crack-arrest specimens at BCL, but BCL has since then decommissioned their hot cell facilities. Nine irradiated crack-arrest specimens have been tested at ORNL and preliminary results were reported previously.[2]

The CMOD measurement was originally intended to be performed using a clip gage designed to be seated on knife edges located on the front face of the specimen. At ORNL, the CMOD of crack-arrest specimens is measured using clip gage blocks with conical recesses that receive the conical points of the clip gage. According to ASTM E 1221-88, the CMOD should be measured at a distance of 0.25W from the load line and on the opposite side of the crack tip, where W is the nominal width of the specimen. Since ORNL has considerable experience with the conical points clip gage, after consultations with all interested parties, it was decided to use the ORNL method. Clip gage blocks were designed, manufactured, and remotely attached to the ANPA specimens. The CMOD measurements were made at distances of 0.29 and 0.27W in the small and large specimens, respectively, rather than the 0.25W location prescribed in the crack-arrest standard. Hence, the measured CMOD values were greater than those that would have been measured at the recommended distance. To calculate K_{Ia} using the expressions given in ASTM E 1221-88, the measured displacements were adjusted to values that would have been measured at a distance of 0.25W using the method described below.

2.2 Adjustment of the Measured Crack-Mouth Opening Displacements

The method to estimate the required adjustment uses the experimentally measured CMODs and those determined analytically by Newman.[3] Newman has calculated the crack-line displacements for a crack-line wedge-loaded specimen whose geometry corresponds to the ASTM specimen, i.e., one for which 2H/W = 1.2, where 2H is the total specimen height, and W is the nominal width. Plane stress conditions and a Poisson's ratio of 0.3 were assumed. The crack-line displacements were calculated by Newman at several locations from the load-line (LL).

Two of these distances are 0.25 and 0.1576W, where W is the nominal specimen width that corresponds to the distance from the LL to the back face of the specimen. The 0.25W location corresponds to that prescribed in ASTM E 1221-88.

It is assumed that the crack-line displacements, at locations from the LL to beyond the front face of the specimen, are approximately linear.* By using similar triangles, the following relationship may be written:

$$\frac{V_M - V_o}{M - 0.25} = \frac{V_o - V_1}{0.25 - 0.1576}, \tag{2.1}$$

where V_M, V_0, and V_1 are one-half the crack-line displacement at locations M, 0, and 1, respectively, (see Figure 2.1). Using Newman's nomenclature,[3] location 0 is at the front face (at 0.25W), and 1 is at 0.1576W. The conical recess of the clip gage blocks is located at M and is thus the point at which the CMODs were measured in the ANPA specimens. It is 3.2 mm away from the front face of the specimen and results in CMODs measured at distances of 0.29 and 0.27W for the small and large specimens, respectively, rather than the 0.25W prescribed in ASTM E 1221-88. Solving for the front-face displacement V_0, Equation (2.1), becomes:

$$V_o = \frac{0.0924V_M + V_1 (M - 0.25)}{0.0924 + (M - 0.25)} \tag{2.2}$$

ORNL-DWG 94-13363

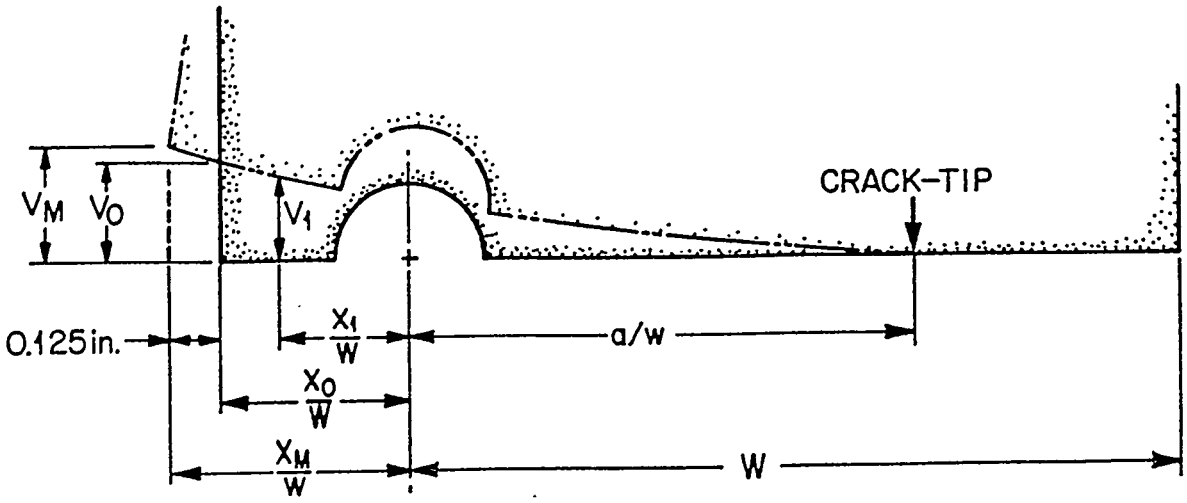

Figure 2.1. Locations M, 0, and 1 at which one-half of the crack-line displacement V_M, V_o, V_1, respectively, were calculated.

*This is approximately true, as can be seen in Figure 11 of reference 3, since this part of the specimen is not subjected to any loads.

The crack-line displacements given by Newman are normalized with respect to the applied force, P, and are thus the specimen compliances at the respective locations. These compliances, C, are of the form:

$$C = \frac{2EBV}{P} \quad , \tag{2.3}$$

where B is the specimen thickness, and E is Young's Modulus. Solving for the displacement V yields:

$$V = \frac{CP}{2EB} \quad . \tag{2.4}$$

To account for the side grooves, the correction to the above expression can be multiplied by a square root term as follows:

$$V = \frac{CP}{2EB}\sqrt{\frac{B}{B_n}} \quad , \tag{2.5}$$

where B_N is the specimen thickness at the root of the side groves. The correction term can also be of the form (B/B_e) where B_e is from ASTM "Standard Test Method for Determining J-R Curves" (E 1152-87):

$$B_e = B - \frac{(B - B_n)^2}{B} \tag{2.6}$$

It should be noted that either form gives the same value for the adjusted CMOD, since the compliances are only used to interpolate for the front-face CMOD, but the opening force, P, is about 10% higher when (B/Be) is used rather than the square root term.

The specimen compliances at locations 0 and 1, excerpted from Newman's reference, are given in Table 2.1. To interpolate the compliances at crack lengths other than those tabulated, the following function was regression fit to the tabulated values:

$$C^{0.5} = A + \frac{B}{\ln \frac{a}{W}} \quad , \tag{2.7}$$

where A and B are parameters, and a is the crack length. The parameters A and B are given in Table 2.2, and the resulting fits are shown in Figure 2.2. The form of Equation 2.7 was chosen as the simplest from a large number of other trial candidate equations.

Table 2.1. Normalized crack-line displacements at specimen front face, x = 0.25W, and at x = 0.1576W as a function of crack length (plane stress conditions and Poisson's ratio = 0.3 were assumed)

Normalized crack length (a/W)	Normalized crack-line displacement at x = 0.25W ($2EBV_0/P$)	Normalized crack-line displacement at x = 0.1576W ($2EBV_1/P$)
0.20	12.18	11.15
0.25	15.64	14.26
0.30	19.90	18.14
0.35	25.12	22.80
0.40	31.58	28.64
0.45	39.73	36.05
0.50	50.33	45.70
0.55	64.59	58.73
0.60	84.63	77.07
0.65	114.30	104.20
0.70	161.00	147.20
0.75	240.80	220.60
0.80	392.40	360.20

Source: Excerpted from Table III, J. C. Newman, Jr., *Crack-Opening Displacements in Center-Crack, Compact, and Crack-Line Wedge-Loaded Specimens*, NASA TN D-8268, NASA Langley Research Center, July 1976.

Table 2.2 Results of regression fitting Equation (2.7) to the compliances at positions 0 and 1 for various crack lengths

Position	A	B
0 front face	0.977	–4.196
1 intermediate	0.888	–4.0299

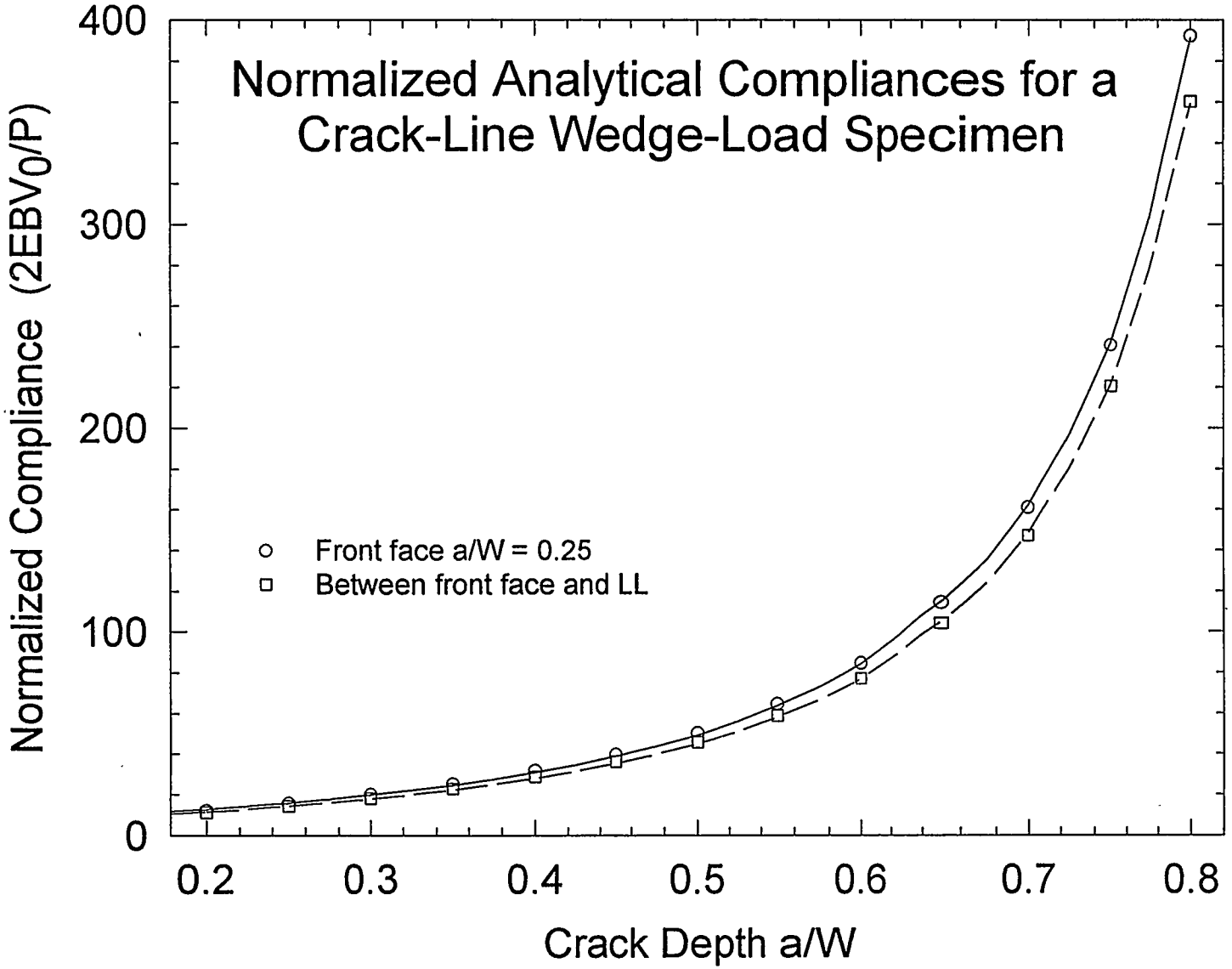

Figure 2.2 **Crack-line wedge-loaded specimen compliances and regression fit of Equation (2.7) *Source*: J. C. Newman, Jr., *Crack-Opening Displacements in Center-Crack, Compact, and Crack-Line Wedge-Loaded Specimens,* NASA TN D-8268, NASA Langley Research Center, July 1976.**

The opening force, P, applied to the LL is not directly known from the experiment, since the load recorded during the crack-arrest test is the wedge load and includes various friction forces, such as that between the wedge and the split pins. However, it can be deduced iteratively from the above relations using the following algorithm for each arrested crack depth, aa / W:

1. Estimate the force P.

2. Calculate the CMODs, V_0, and V_1, at locations 0 and 1 using Newman's compliances, interpolated for the arrested crack depth of the specimen.

3. Interpolate for the front-face CMOD, V_0', using Equation (2.2) and using the measured value, V_M, and the CMOD at location 1, V_1, calculated in step 2.

4. Compare V_0' and V_0, and adjust the P until $(V_0' - V_0)/V_M$ is $\leq 0.1\%$.

The results of the above calculations are shown in Table 2.3. It may be seen that the relative difference between the measured values and the adjusted ones $[(V_m' - V_0)/V_M]$ is < 4 % for the smaller and < 2% for the larger specimens. These adjustments were also estimated by assuming that the rotation point for the specimens is at the crack tip and were approximately the same as those obtained using the above procedure. However, the errors of this latter procedure would not have been known.

References

1. P. P. Milella, A. Pini, and C. W. Marschall, "Radiation Effects on the Mechanical Properties of SA 508 Cl. 3 Forging," pp. 227-37 in Radiation Embrittlement of Nuclear Pressure Vessel Steels: An International Review (Fourth Volume), ASTM STP 1170, ed. L. E. Steele, American Society for Testing and Materials, Philadelphia, 1993.*

2. S. K. Iskander et al., Martin Marietta Energy Systems, Inc., Oak Ridge Natl. Lab., "Fracture Toughness Shift in High-Copper Weldments," in Heavy-Section Steel Irradiation Program Semiannual Progress Report April-September 1994, USNRC Report NUREG/CR-5591, Vol. 5, No. 2 (ORNL/TM-11568/V5&N2), 1995.†

3. J. C. Newman, Jr., Crack-Opening Displacements in Center-Crack, Compact, and Crack-Line Wedge-Loaded Specimens, NASA TN D-8268, NASA Langley Research Center, July 1976.†

*Available in public technical libraries.

†Available for purchase from National Technical Information Service, Springfield, VA 22161.

Table 2.3. Details of calculations to adjust the measured crack-mouth opening displacement to account for > 0.25W location at which they were measured

Specimen ID	a/W	Co	C1	E (ksi)	2VM (mils)	P (kips)	B (in.)	Bn (in.)	Calculated from compliances					
									XmW	2Vo (mils)	2V1 (mils)	2Vo'	(Vo'-vo)/ Vm	(VM-Vo) /VM
BK7	0.62	93.16	85.00	29821	34.5	9.884	0.492	0.378	0.290	33.16	30.26	33.19	0.1%	3.7%
BK8	0.64	105.79	96.59	28921	34.5	8.706	0.492	0.378	0.290	33.17	30.29	33.20	0.1%	3.7%
BK9	0.59	81.12	73.96	29722	31.4	10.308	0.492	0.378	0.290	30.21	27.55	30.25	0.1%	3.8%
BK10	0.59	80.53	73.42	29639	35.8	11.814	0.492	0.378	0.290	34.47	31.43	34.51	0.1%	3..8%
BK11	0.62	92.62	84.51	29556	29.2	8.337	0.492	0.378	0.290	28.06	25.60	28.09	0.1%	3.7%
BK12	0.63	100.28	91.54	29639	28.3	7.485	0.984	0.770	0.270	27.20	24.83	27.22	0.1%	3.7%
BL13 retest	0.77	283.66	260.05	29383	88.1	15.823	0.984	0.770	0.270	86.41	79.22	86.50	0.1%	1.9%
BK16 pop-in	0.68	138.26	126.41	29639	64.0	23.409	0.984	0.770	0.270	62.73	57.35	62.79	0.1%	1.9%
BK16 final	0.90	1790.91	1648.04	30053	82.8	2.376	0.984	0.770	0.270	81.32	74.83	81.40	0.1%	1.9%
BK18	0.66	121.24	110.78	29639	66.4	27.715	0.985	0.770	0.270	65.12	69.50	65.19	0.15	1.9%

3. Fracture Toughness Curve Shift in Low Upper-Shelf Welds (Series 8)

S. K. Iskander, R. K. Nanstad, D. D. Randolph,* and E. T. Manneschmidt

This task examines the fracture toughness curve shifts and changes in shape for irradiated welds with low CVN upper-shelf energy (USE). This task was specifically designed to address questions raised by the Advisory Committee for Reactor Safeguards concerning the shape of the K_{IC} curve for irradiated welds with a low USE. In particular, it will clarify whether the high concentration of inclusions in low-USE welds results in a transition relationship and behavior significantly different from high-USE welds. The information developed under this task will augment information obtained from other HSSI tasks performed on two high-USE weldments under the Fifth and Sixth Irradiation Series and on a commercial, low USE under the Tenth Irradiation Series. The results will provide an expanded basis for accounting for irradiation-induced embrittlement in RPV materials.

Three low-USE welds have been ordered from ABB-Combustion Engineering (ABB-CE), Chattanooga, Tennessee, and two of them have been delivered to ORNL. ABB-CE fabricated the welds for the Fifth and Sixth Series. Preliminary results of mechanical and chemical tests from these two welds are presented below. The Linde 80 flux was used for all three welds. One weld, Weld 1, was made with the 73W weld wire. Weld wire 73W had copper added to the melt to reduce the variations that are associated with copper-coated weld wire. The other two welds were fabricated with a commercially available copper-coated weld wire, L-TEC 44 heat 44112. One of these two welds, Weld 2, has a target copper level of 0.31 %. This copper level could not be attained using the copper-coated wire, and the coating will be stripped from the wire, which contains 0.07 % Cu. To attain the target copper level, supplemental copper will be added to the weld puddle using an ABB-CE proprietary process. This will slightly delay the delivery of weld 2, the expected delivery date is now the end of April 1995. Weld 3 was fabricated with the same heat of the L-TEC 44 copper-coated weld wire as weld 2, but with supplemental copper added to the weld puddle, which resulted in a weldment containing an average of 0.424 % Cu. The semiannual report[1] for October 1993 through March 1994 discusses the reasons for the above choices of copper content and welding wire.

Welds 1 and 3 have been delivered to ORNL, and the results of chemical analyses at different depths through the thickness are given in Tables 3.1 and 3.2. Table 3.3 gives the mechanical properties of welds 1 and 3 as well as the properties of HSSI weld 73 W. It should be noted that all three welds have been postweld heat treated at 607°F (1125°C) for 40 h. Except for the CVN impact energy properties, the remaining mechanical properties do not differ substantially from those of HSSI weld 73W. Figure 3.1 shows the CVN impact energy for welds 1 and 3 together with that of weld 73W. The welds fabricated with Linde 80 flux s have ~ 15% lower USE than the weld 73W fabricated with Linde 124 flux. The transition temperatures of welds 1 and 3 at energy levels of 27, 41, and 68 J (20, 30, and 50 ft-lb) are also significantly higher than those of weld 73W. This is probably due to differences in impurity levels in the weldments, e.g., phosphorous and sulfur, as well as the influence of the two fluxes. Table 3.4 summarizes the average chemical composition of all three welds.

The CVN impact energy of welds 1 and 3 shown in Figure 3.1 is based on testing 14 specimens from each weldment. The specimens were machined from a single depth below the top of the weld after the temper bead weld layer had been sawed off. Plans are to perform more CVN impact testing to get a better statistical basis for welds 1 and 3 and, in particular, the USE (the CVN impact energy curve for weld 73W is based on 85 specimens). Also, the initiation fracture toughness in the transition region for these welds 1 and 3 will be determined.

An evaluation of welds 1 and 3 will be performed so that one or possibly two welds can be chosen for fabrication in sufficient quantities for the HSSI Eight and Ninth Series. To estimate the linear feet of weld needed for the Eight and Ninth Series, a detailed test plan must first be developed, particularly with regard for the thickness of the compact tension specimens. A sufficiently thick compact tension specimen is required so that the toughness at

*ABB-Combustion Engineering, Chattanooga, Tennessee.

Table 3.1. Results of chemical analysis through the thickness of weld 1 (fabricated with weld wire 73W using Linde 80 flux with copper added to the melt)

Element	weight percent at distance from top of weld					Average (wt %)	Standard deviation (wt %)
	25 mm	64 mm	108 mm	152 mm	191 mm		
Carbon	0.096	0.097	0.091	0.089	0.087	0.092	0.0044
Manganese	1.630	1.630	1.690	1.680	1.700	1.666	0.0336
Phosphorus	0.007	0.009	0.008	0.008	0.007	0.008	0.0008
Sulfur	0.006	0.007	0.006	0.006	0.006	0.006	0.0004
Silicon	0.34	0.35	0.36	0.35	0.38	0.356	0.0152
Nickel	0.59	0.59	0.61	0.61	0.60	0.600	0.0100
Chromium	0.25	0.24	0.25	0.25	0.25	0.248	0.0045
Molybdenum	0.53	0.53	0.56	0.56	0.56	0.548	0.0164
Vanadium	0.003	0.003	0.003	0.003	0.003	0.003	0.0000
Niobium	0.003	0.003	0.003	0.003	0.004	0.003	0.0004
Titanium	0.002	0.002	0.002	0.002	0.000	0.002	0.0009
Cobalt	0.028	0.028	0.030	0.030	0.030	0.029	0.0011
Copper	0.30	0.30	0.32	0.32	0.32	0.312	0.0110
Aluminum	0.006	0.006	0.006	0.006	0.006	0.006	0.0000
Boron	0.001	0.001	0.001	0.001	0.001	0.001	0.0000
Tungsten	0.01	0.01	0.01	0.01	0.01	0.01	0.0000
Arsenic	0.004	0.005	0.005	0.005	0.005	0.005	0.0004
Tin	0.004	0.004	0.004	0.004	0.004	0.004	0.0000
Zirconium	0.001	0.001	0.001	0.001	0.001	0.001	0.0000

Table 3.2 Results of chemical analysis through the thickness of weld 3 (fabricated with commercial copper-coated weld wire using Linde 80 flux))

Element	weight percent at distance from top of weld					Average (wt %)	Standard deviation (wt. %)
	25 mm	64 mm	108 mm	152 mm	191 mm		
Carbon	0.091	0.083	0.079	0.086	0.082	0.084	0.0046
Manganese	1.73	1.71	1.72	1.65	1.72	1.706	0.0321
Phosphorus	0.015	0.015	0.015	0.014	0.015	0.015	0.0004
Sulfur	0.011	0.011	0.011	0.011	0.010	0.011	0.0004
Silicon	0.39	0.39	0.42	0.40	0.38	0.396	0.0152
Nickel	0.61	0.60	0.60	0.58	0.60	0.598	0.0110
Chromium	0.08	0.09	0.09	0.09	0.08	0.086	0.0055
Molybdenum	0.44	0.43	0.43	0.42	0.43	0.430	0.0071
Vanadium	0.003	0.003	0.003	0.003	0.003	0.003	0.0000
Niobium	0.003	0.004	0.004	0.003	0.003	0.003	0.0005
Titanium	0.002	0.002	0.002	0.002	0.002	0.002	0.0000
Cobalt	0.011	0.011	0.011	0.011	0.011	0.011	0.0000
Copper	0.42	0.41	0.41	0.43	0.43	0.424	0.0089
Aluminum	0.007	0.008	0.008	0.007	0.007	0.007	0.0005
Boron	0.001	0.001	0.001	0.001	0.001	0.001	0.0000
Tungsten	0.01	0.01	0.01	0.01	0.01	0.010	0.0000
Arsenic	0.007	0.007	0.007	0.006	0.006	0.007	0.0000
Tin	0.013	0.013	0.014	0.013	0.013	0.013	0.0004
Zirconium	0.001	0.002	0.002	0.001	0.001	0.001	0.0005

Table 3.3. Mechanical properties of welds 1 and 3 fabricated with Linde 80 flux compared to HSSI weld 73W fabricated with Linde 124

[all postweld heat treated at 607°C (1125°F) for 40 h]

Flux	Linde 124	Linde 80	
Wire	73W	73W	L-TEC 44 (heat 44112)
Copper (wt %)	0.31	0.312	0.424
Yield strength (MPa)	495	521	516
Ultimate strength (MPa)	606	630	613
Drop-weight nil-ductility transition (°)	-34	-29	-34
Upper-shelf energy (J)	135	114	117
Temperature (°C) at energy levels of:			
27 J (20 ft-lb)	-54	-30	-25
41 J (30 ft-lb)	-40	-19	-8
68 J (50 ft-lb)	-18	-1	-19

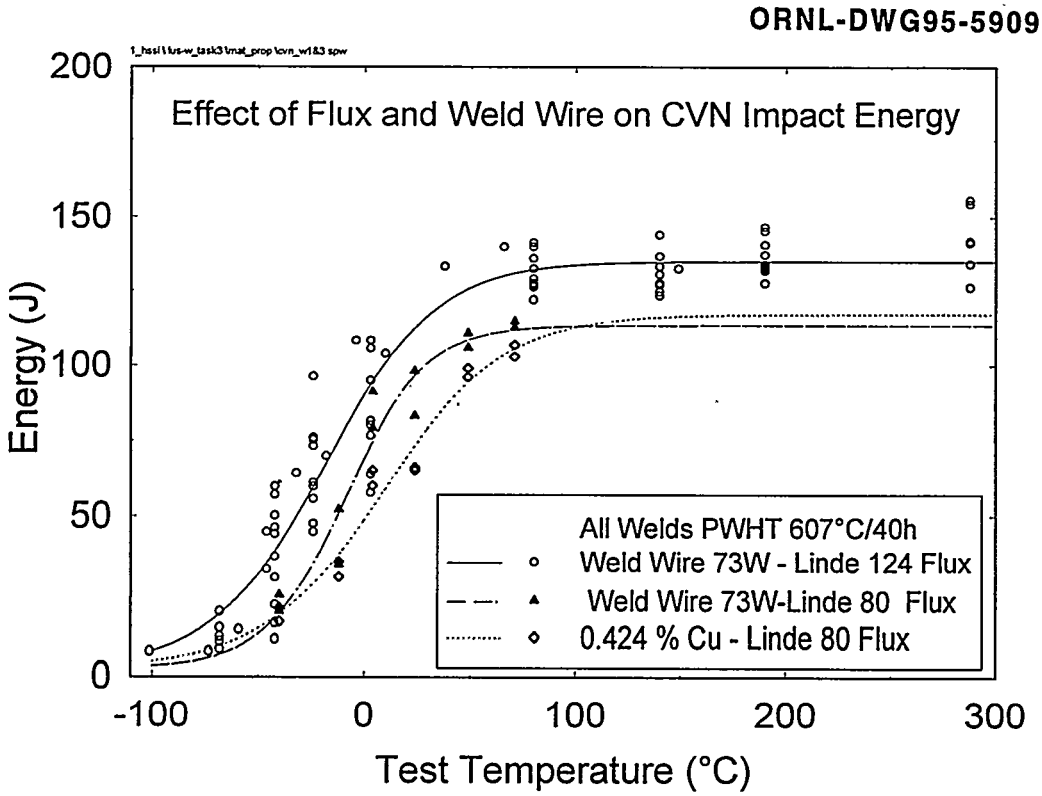

Figure 3.1. Comparison of the Charpy V-notch impact energy for welds 1 and 3 to HSSI weld 73W.

Table 3.4. Comparison of chemical composition of weld 73W (Linde 124 flux) and welds 1 and 3 (L-TEC heat 44112 and Linde 80 flux)

Weld	Composition (wt %)									
	C	Mn	P	S	Si	Cr	Ni	Mo	Cu	V
73W	0.098	1.56	0.005	0.005	0.45	0.25	0.60	0.58	0.31	0.003
Weld 1	0.092	1.666	0.008	0.006	0.356	0.248	0.600	0.548	0.312	0.003
Weld 3	0.084	1.706	0.015	0.011	0.396	0.396	0.598	0.430	0.424	0.003

high-USE levels can be defined, which is necessary to determine whether the shape of the toughness curve in the transition region changes due to irradiation. The development of the new test practice for fracture toughness in the transition region is very promising, since it appears to give a more accurate transition temperature shift at the 100-MPa•√m level using 25-mm-thick compact tension [1T (C(T)] specimens, perhaps even with specimens as small as 0.5 T C(T). However, in order to determine the possible changes in slope, a specimen with a capacity of 150 to 200 MPa•√m is needed, which may require a 2T C(T) specimen. The results from the ongoing Tenth Irradiation Series, which investigates a commercial low-USE weld, will also be taken into account in planning the HSSI Eighth and Ninth Series.

References

1. S. K. Iskander, E. T. Manneschmidt, and K. W. Boling, Martin Marietta Energy Systems, Inc., Oak Ridge, Natl. Lab., "K_{Ia} Curve Shift in High-Copper Welds," in *Heavy-Section Steel Irradiation Program Semiannual Progress Report October 1993—March 1994*, USNRC Report NUREG/CR-5591, Vol. 5, No. 1 (ORNL/TM-11568/V5&N1), 1995.*

*Available for purchase from the National Technical Information Service, Springfield, VA 22161

4. Irradiation Effects in a Commercial Low Upper-Shelf Weld (Series 10)

D. E. McCabe, S. K. Iskander, I. I. Siman-Tov, and D. W. Heatherly

4.1 Introduction

The objective of this task is to evaluate the transition temperature shift of the WF-70 weld material at the beltline and nozzle course locations in the Midland reactor vessel. This material is classified as an LUS weld material, and the fracture toughness is to be characterized in the as-received condition as well as three levels of irradiation fluence, 0.5, 1.0, and 5.0×10^{19} neutrons/cm^2. A complete survey of the material chemistries and mechanical properties has been made in the unirradiated condition.

4.2 Transition Temperature Characterization

CVN transition temperature curves of unirradiated weld metal were generated at 19 positions throughout the beltline weld and at 6 positions throughout; the nozzle course weld. Each was independently evaluated for reference temperature (RT_{NDT}). The results was variability in transition temperature characterization for the beltline weld that ranged from -20 to 37°C and from -8 to 18°C for the nozzle course weld. When the CVN data from all positions were combined into one plot (Figure 4.1), the curves based on the median were nearly the same between the two welds. The USE was just about identical at 88 J (65.3 ft-lb) as well. DWT NDT tests tended to confirm the similarity of unirradiated transition temperature, nominally at -55°C (-67°F) for both welds.

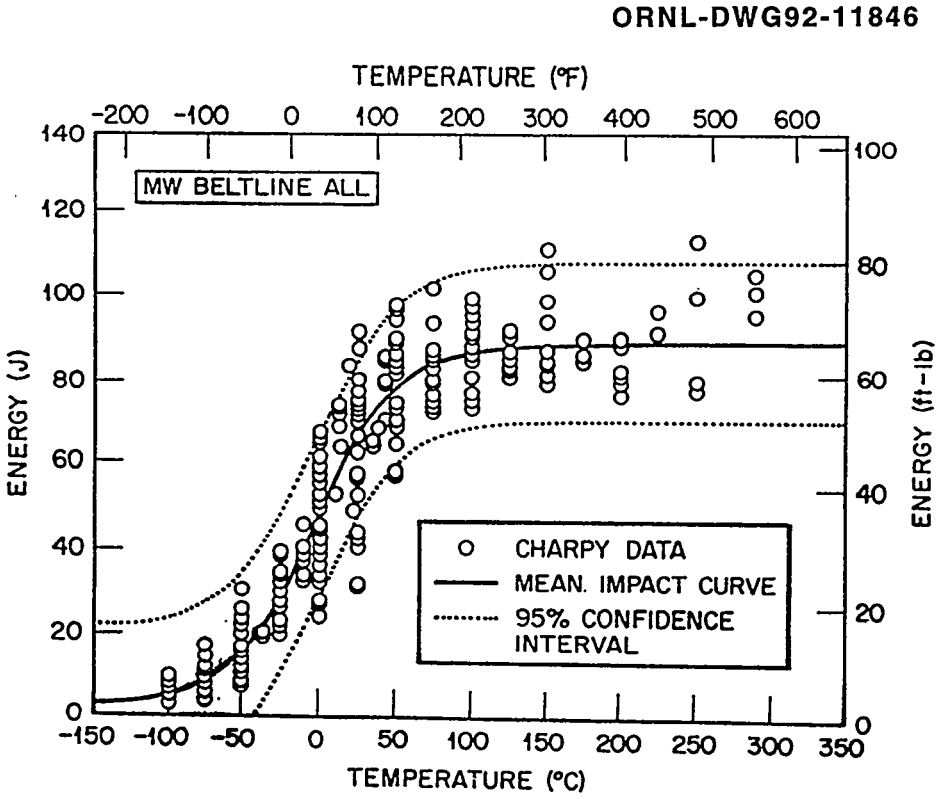

Figure 4.1 **Combined Charpy V-notch data taken around the girth and from several through-thickness positions of the beltline weld.**

CVN specimens of beltline and nozzle course weld material were irradiated in separate capsules (scoping capsules 10.01 and 10.02) to 0.5×10^{19} neutrons/cm^2 (< 1 MeV). Other groups of CVN specimens of both welds were irradiated in a larger capsule (capsule 10.05) to 1×10^{19} neutrons/cm^2 (< 1 MeV). In all cases, the number of specimens was reduced, compared to the unirradiated tests, to 14 to 24 CVN specimens per condition, so the data scatter characteristics could not be well characterized. The Charpy curves for the specimens irradiated in capsule 10.05 are shown in Figures 4.2 and 4.3. The summary of the 41-J transition temperature shifts is given in Table 4.1.

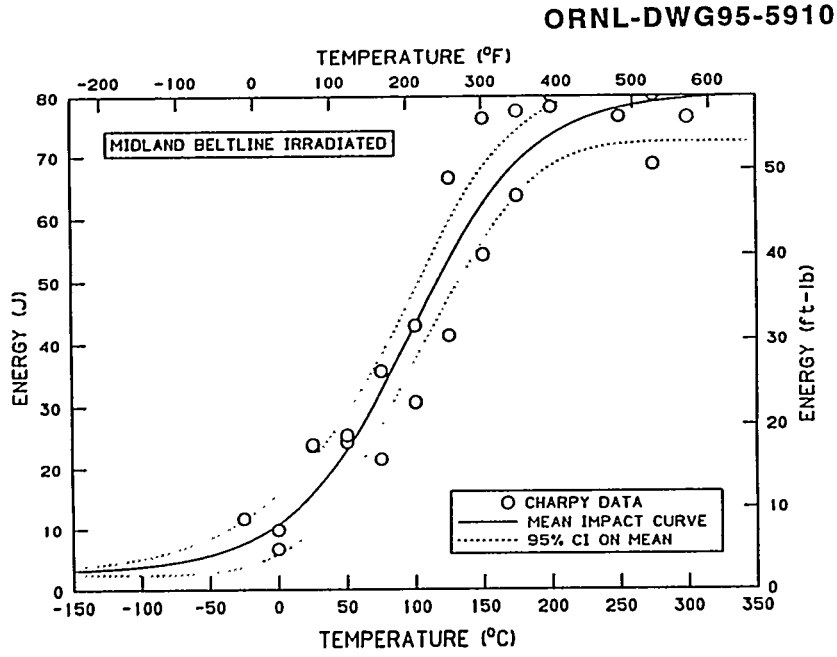

Figure 4.2. Charpy V-notch energy transition temperature curve for beltline weld metal irradiated in capsule 10.05 (1×10^{19} neutrons/cm^2).

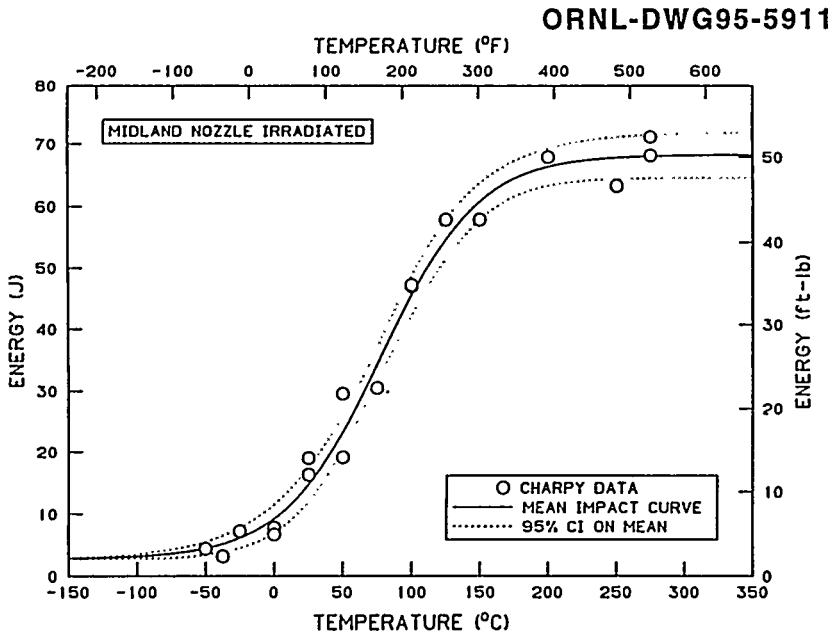

Figure 4.3 Charpy V-notch energy transition curve for nozzle course weld metal irradiated in capsule 10.05 (1×10^{19} neutrons/cm^2).

Table 4.1 Summary of 41-J transition temperature shifts for beltline and nozzle course weld metal

Condition	ΔTT_{41J}		Upper-shelf energy	
	(°C)	(°F)	(J)	(ft-lb)
Beltline weld				
Unirradiated	0	0	88	65
0.5×10^{19} neutrons/cm^2	43	78	82	60
1×10^{19} neutrons/cm^2	104	187	81	59
Nozzle course weld				
Unirradiated	0	0	89	65
0.5×10^{19} neutrons/cm^2	66	118	71	52
1×10^{19} neutrons/cm^2	92	166	69	50

The trend in Charpy curve shift with irradiation damage for the two fluence levels is shown in Figures 4.4 and 4.5 Other than copper content, the chemistries of the two weld metals are identical. Therefore, these figures suggest that the kinetics of damage development is sensitive to copper content.

4.3 Transition Temperature Effects by Fracture Mechanics Evaluations

Fracture mechanics-type data have been available for the unirradiated condition of both beltline and nozzle course welds. It was determined that the transition range toughness expressed as K_{Jc} values is well modeled by a master curve.[1] The master curve defines the transition range toughness for each weld metal when tested as 1T compact specimens (Figure 4.6). The transition temperature shift due to damage mechanisms is keyed to the reference temperature , T_o, that corresponds to K_{Jc} = 100 MPa$\sqrt{m}$ (90.9 ksi$\sqrt{in.}$). Reference temperature shift information is available for beltline weld metal only at the present time. Table 4.2 is a preliminary listing of the reference temperatures.

4.4 Evaluation of Reference Toughness Methods

Since it is now possible to place pseudostatic fracture toughness (using fracture mechanic methods) more accurately with the master curve method, it is also possible to benchmark the ASME methods currently in use.

Because WF-70 is a low-USE material, the RT_{NDT} temperature is established from CVN transition curves. For the beltline weld, the average initial RT_{NDT} from the 19 individual determinations was 8°C (46°F). The transition temperature shift is also dependent on the Charpy curve at the 41-J (30-ft-lb) level, and 1×10^{19} neutrons/cm^2, the beltline ΔTT_{41J} was 104°C (187°F). This information is used to establish the positions on the abscissa (temperature axis) for the lower-bound K_{Ic} curve. If there is absolutely no fracture toughness information available, the K_{Ic} curve can be positioned using generic information and correlations between Charpy shifts, ΔTT_{41J}, chemistry, and fluence/damage plots. Such predictions require a larger margin to maintain sufficient conservatism. Table 4.3 lists reference temperatures for the WF-70 beltline weld metal. The maximum allowable RT_{NDT} for weld metals is 132°C (270°F) by the *Code of Federal Regulations* (10CFR50).[2]

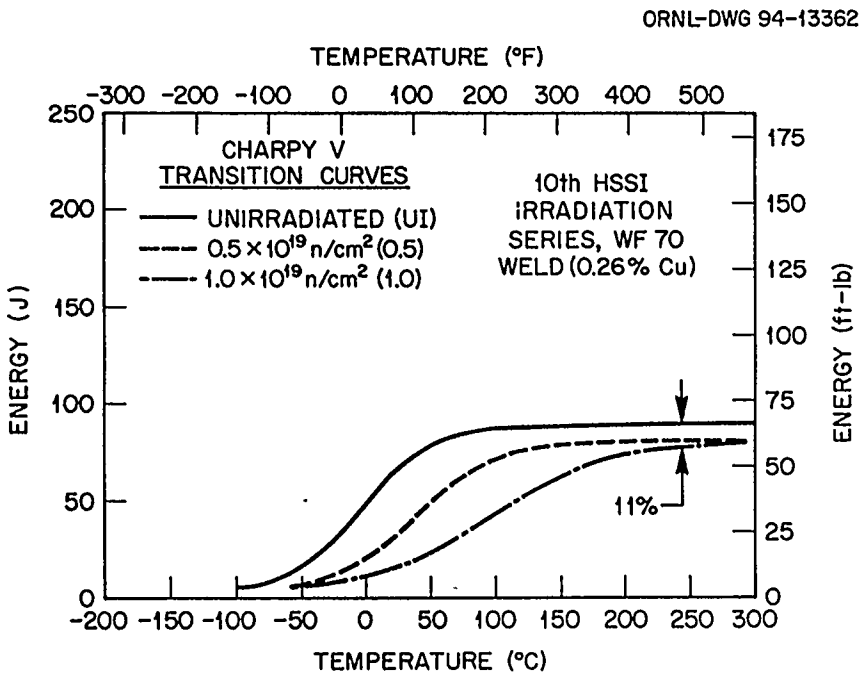

Figure 4.4. Trend in Charpy V-notch energy transition curve of Midland beltline weld metal, comparing as-recieved, 0.5 × 10^{19} neutrons/cm^2, and 1 × 10^{19} neutrons/cm^2 irradiation damage levels.

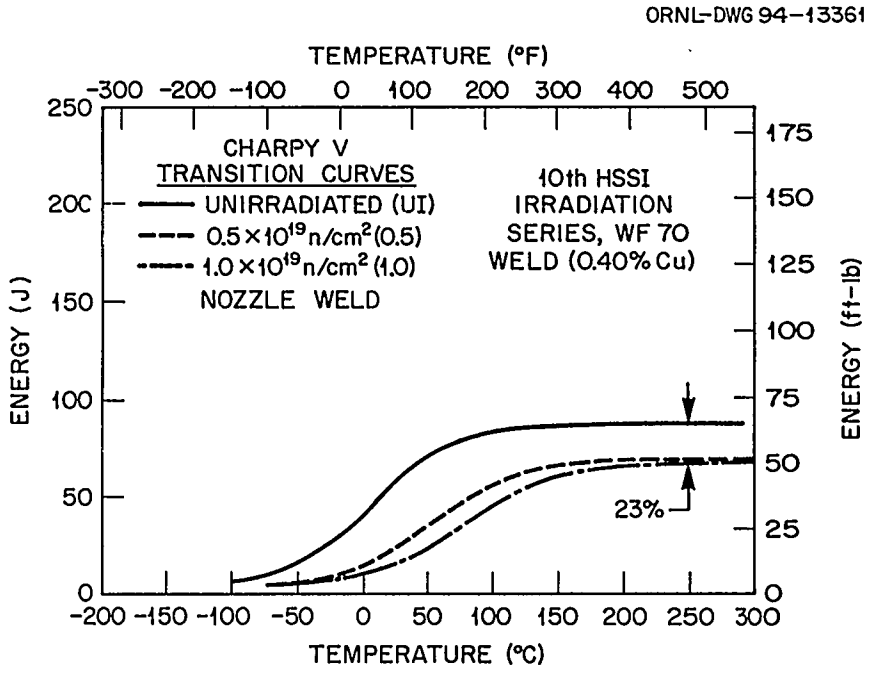

Figure 4.5. Trend in Charpy V-notch energy transition curve of Midland nozzle course weld metal, comparing as-recieved, 0.5 × 10^{19} neutrons/cm^2, and 1 × 10^{19} neutrons/cm^2 irradiation damage levels.

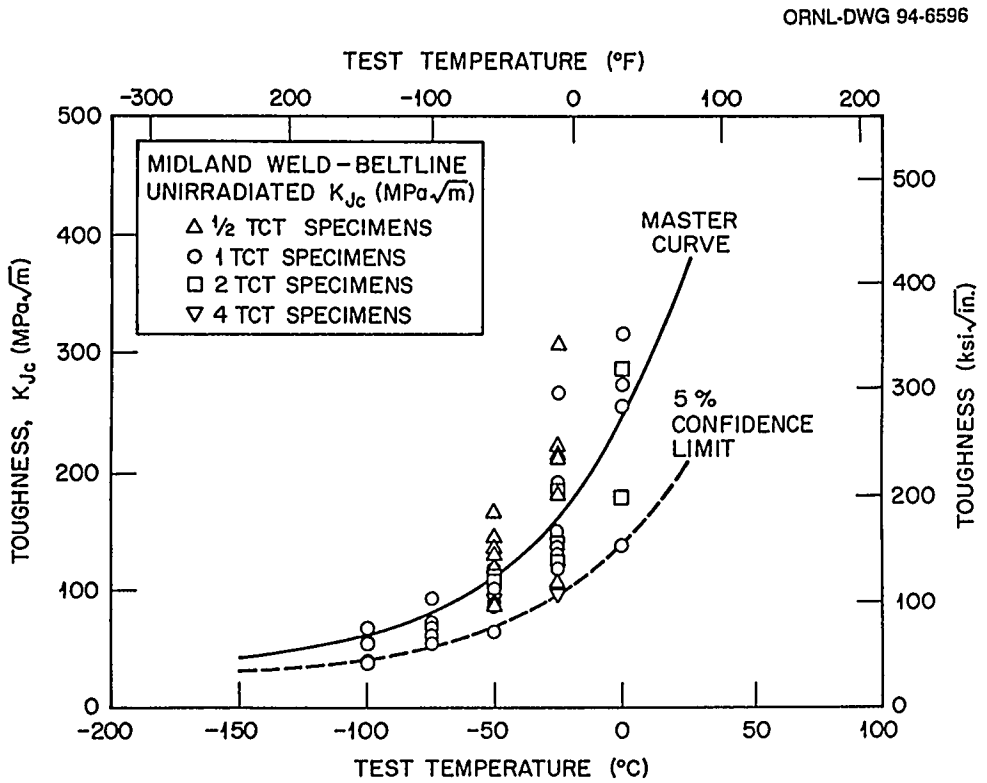

Figure 4.6. Master curve (T_o = -60°C) and experimental data for unirradiated Midland beltline weld metal. The confidence limit curve results from the known standard deviation of the data scar.

Table 4.2. Reference temperatures, T_o

Condition	Temperature (°C)	Temperature (°F)
Beltline weld		
Unirradiated	−60	−76
0.5×10^{19} neutrons/cm^2	22	72
1×10^{19} neutrons/cm^2	35	95
Nozzle course weld		
Unirradiated	−34	−29
0.5×10^{19} neutrons/cm^2	*a*	*a*
1×10^{19} neutrons/cm^2	*a*	*a*

[a]Not yet available.

Table 4.3. Transition curve shift of beltline WF-70 weld due to irradiation to 1 × 10^{19} neutrons/cm^2

	RT_{NDT} (°C)	1 ×10^{19} neutrons/cm^2		
		ΔTT	ΔTT + margin	A RT_{NDT}[a]
Generic	−18	97.5	134.2	116
ASME	8	104	135.1	143
T_o	−60	95	95[b]	35[b]

[a]Adjusted reference temperature.
[b]10°C margin added lower-bound confidence limit only.

Figure 4.7 contains fracture mechanics data (all normalized to 1T compact specimen size) that puts the fracture toughness estimations into perspective. The two ASME lower-bound K_{Ic} curves are positioned very conservatively. The 5% lower-bound curve on the master curve data has been offset by only a 10°C margin. Failure to meet 10CFR50 requirements on LUS weldments does not appear to portend a dangerous material fracture toughness condition.

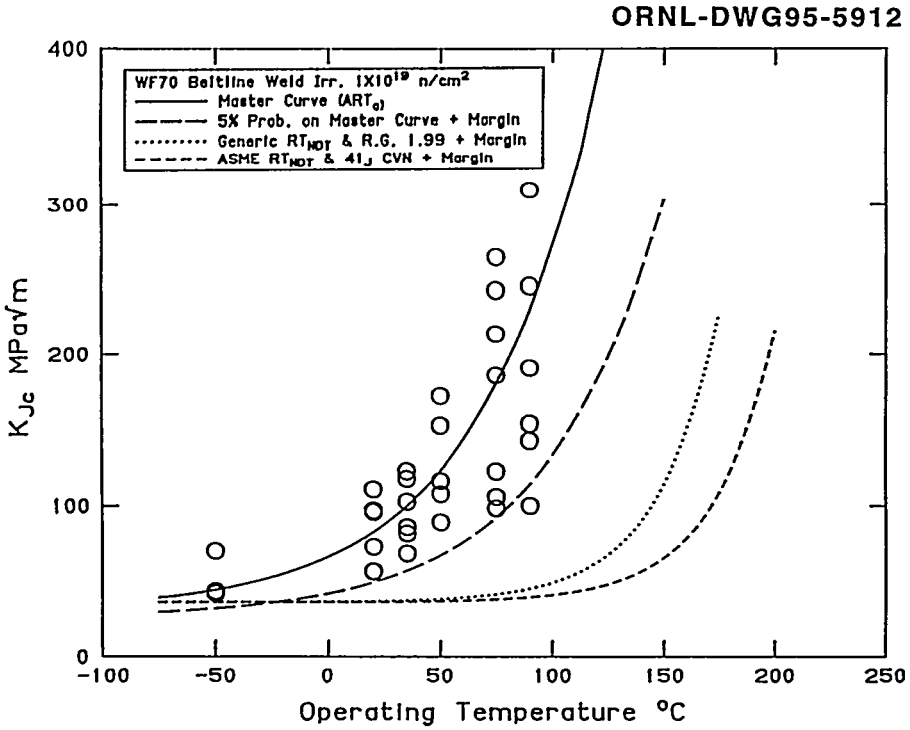

Figure 4.7. Analyses of Midland beltline weld data and three lower-bound curves

4.5 Fracture Mechanics Data from Charpy Specimens

Recently, there has been some interest in using Charpy specimens to replace the much larger fracture mechanics specimens to obtain valid K_{Jc} values. Statistical methods that have been developed to model specimen size effects (weak-link theory) have opened the door to the above possibilities.

One such possibility that has been suggested is to relate crack-arrest events often seen in autographic load-time traces during the standard CVN impact tests to K_{Ia} transition curves. The following correlation equation has been proposed by Wallin[3] that relates crack-arrest load of Charpy specimens to a valid crack-arrest K_{Ia} value of 100 MPa$\sqrt{m}$:

$$T_{(100)Ia} = T_{F4} - 10 \quad °C \ .$$

Variable T_{F4} is the temperature where the Charpy records show an arrest load, P_a, to be 4 kN. The technique of determining T_{F4} is to plot arrest loads obtained throughout the transition range.

Figure 4.8 contains the plot for the WF-70 beltline weld metal before and after irradiation. The shift in K_{Ia} transition appears to be only about one-half of the 41-J transition temperature shift. Large specimens believed to be capable of producing valid ASTM K_{Ia} values are available to check this result.

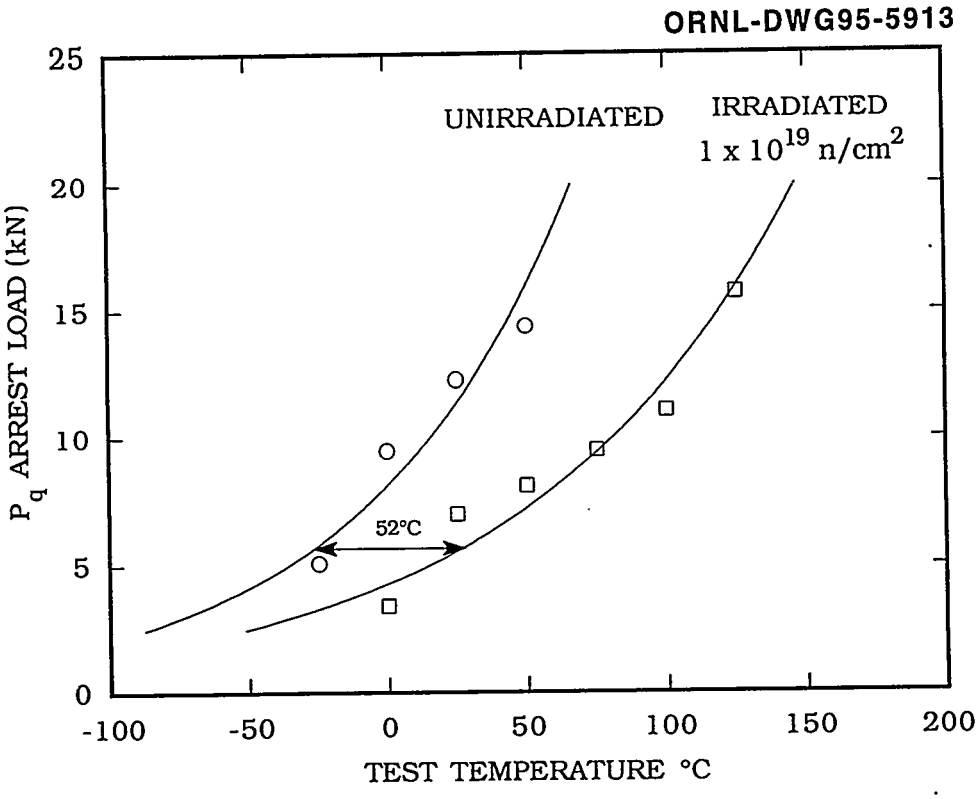

Figure 4.8. Crack-arrest loads obtained from CVN autographic load-time traces on beltline weld metal before and after irradiation to 1 × 10^{19} neutrons/cm^2.

Another possibility for the use of Charpy specimens that is currently being explored is to use precracked specimens and test them as fracture mechanics three-point bend bars. The Charpy bend bar that is fatigue precracked to 50% of the depth is, in fact, a miniature specimen but of highly limited K_{Jc} capacity. A proposed ASTM test practice currently under development was used to obtain T_o reference temperatures from both beltline and nozzle course weld metals. The conditions were tested before and after irradiation at 1×10^{19} neutrons/cm^2. Table 4.4 lists the values obtained.

Table 4.4. Reference temperatures, T_o, from precracked Charpy specimens

Condition	Temperature (°C)
Beltline weld	
Unirradiated	−59
1×10^{19} neutrons/cm^2	30
Nozzle course weld	
Unirradiated	−60
1×10^{19} neutrons/cm^2	44

Because these were such small specimens with only 5 mm (0.2 in.) of initial remaining ligament, a few of the specimens tested suffered from loss of constraint, and the K_{Jc} values were elevated above an acceptable limit; a data-censoring technique was applied in the analysis of these data. The results from beltline weld metal are compatible with the results from larger fracture mechanics specimens. However, the lower unirradiated fracture toughness of the nozzle course material is not confirmed by the Charpy specimens where the T_o by legitimate and valid K_{Jc} tests was -33°C. The postirradiation T_o temperature for the nozzle course material is not currently known because the irradiation capsule that has the fracture mechanics specimens has not yet been opened.

4.6 Irradiation Capsule Activities

Capsule 10.06 was shipped to ORNL from the Ford Nuclear Reactor (FNR) on January 13, 1995, as planned. The capsule is currently stored in an on-site hot cell in Building 3525. Disassembly has been delayed pending approval to proceed with that particular project tack (Task 4.2).

A preliminary report on the exposure parameters for capsule 10.05 [1×10^{19} neutrons/cm^2 (E> 1 MeV)] has been prepared and is undergoing internal peer review.

References

1. D. E. McCabe, R. K. Nanstad, S. K. Iskander, and R. L. Swain, Martin Marietta Energy Systems, Inc., Oak Ridge Natl. Lab., *Unirradiated Material Properties of Midland Weld WF-70*, USNRC Report NUREG/CR-6249 (ORNL/TM-12777), October 1994.*

2. "Title 10," *Code of Federal Regulations* , Part 50, U.S. Government Printing Office, Washington, D.C., January 1987.†

3. K. Wallin, "A Simple Theoretical Charpy-V K_{Ic} Correlation for Irradiation Embrittlement." pp. 93-100 in *Innovative Approaches to Irradiation Damage and Fracture Analysis*, PVP-Vol. 170, American Society of Mechanical Engineers, New York, 1989.†

*Available for purchase from National Technical Information Service, Springfield, VA 22161.
†Available in public technical libraries.

5. Irradiation Effects on Weld Heat-Affected Zone and Plate Materials (Series 11)

R. K. Nanstad and D. E. McCabe

The purpose of this task is to examine the effects of neutron irradiation on the fracture toughness (ductile and brittle) of the HAZ of welds and of A 302 grade B (A302B) plate materials typical of those used fabricating older RPVs. The initial plate material of emphasis will be A302B steel, not the A302B modified with nickel additions. This decision was made by the NRC following a survey of the materials of construction for RPBs in operating U.S. nuclear plants. Reference 1 was used for the preliminary survey, and the information from that report was revised by NRC staff based on information contained in the licensee responses to Generic Letter (GL) 92-01, "Reactor Vessel Structural Integrity, 10CFR50.54(f)." The resulting survey showed a total of eight RPVs with A302B, ten with A302B (modified), and one with A302 grade A plate. Table 5.1 in the previous semiannual report[1] provides a summary of that survey. For the HAZ portion of the program, the intent is to examine HAZ material in the A302B (i.e., with low nickel content) and in A302B (modified) or A533B-1 (i.e., with medium nickel content).

During this reporting period, two specific plates were identified as being applicable to this task. One plate is A302B and the other is A302B (modified). The A302B plate (43 × 42 × 7 in.) will be prepared for welding, while the A302B (modified) plate already contains a commercially produced weld (heat 33A277, Linde 0091 flux). These plates were identified from a list of ten materials provided by Mr. E. Biemiller of Yankee Atomic Electric Company (YAEC). The materials have been requested from YAEC for use in this irradiation task, and arrangements are being made with YAEC for procurement of the plates mentioned above.

References

1. R. K. Nanstad and D. E. McCabe, Martin Marietta Energy Systems, Inc., Oak Ridge Natl. Lab., "Irradiation Effects on Weld Heat-Affected Zone and Plate Materials (Series 11)," in *Heavy-Section Steel Irradiation Program Semiannual Progress Report April - September 1994*, 1994, USNRC Report NUREG/CR-5591, Vol. 5, No. 2 (ORNL/TM-11568/V5&N2), 1995.*

*Available for purchase from National Technical Information Service, Springfield, VA 22161.

6. Annealing Effects in Low Upper-Shelf Welds (Series 9)

S. K. Iskander and R. K. Nanstad

6.1 Introduction

The purpose of the Ninth Irradiation Series is to evaluate the correlation between fracture toughness and CVN impact energy during irradiation, annealing, and reirradiation (IAR). Results of annealing CVN specimens from the low-USE welds from the Midland beltline and nozzle course welds, as well as HSST plate 02 and HSSI weld 73W are given. Also presented is the effect of annealing on the initiation fracture toughness of annealed material from Midland beltline weld and HSST plate 02. The results from capsule 10-5 specimens of weld 73W confirm those previously obtained on the so-called undersize specimens that were irradiated in the Fifth Irradiation Series, namely that the recovery due to annealing at 343°C (650°F) for 1 week is insignificant.

The fabrication of major components for the IAR facility for two positions on the east side of the FNR at the University of Michigan has begun. Fabrication of two reusable capsules (one for temperature verification and the other for dosimetry verification), as well as two capsules for IAR, studies is also under way. The design of a reusable capsule capable of reirradiating previously irradiated and annealed CVN and 1T C(T) specimens is also progressing. The data acquisition and control (DAC) instrumentation for the first two IAR facilities is essentially complete and awaiting completion of the IAR facilities and temperature test capsule for checkout and control algorithm development.

6.2 Effect of Annealing Irradiated Materials (M. A. Sokolov, R. L. Swain, and J. J. Henry)

The Midland beltline weld specimens irradiated in capsule 10.5 were annealed at 454 and 343°C (850 and 750°F) for 1 week. Figures 6.1 and 6.2 present CVN and fracture toughness properties, respectively, of the Midland beltline weld in the unirradiated, irradiated, and irradiated/annealed conditions. The shift of CVN T_{41J} due to irradiation was 103°C compared to a 92°C shift of fracture toughness reference transition temperature, T_o. Annealing at 343°C for 168 h resulted in full recovery of CVN USE but in only 49% recovery of the transition temperature. The residual shift (nonrecovered after annealing) of the CVN transition temperature (ΔT_{res}) is 53°C. The USE after annealing at 454°C for 168 h increased to 106 J, which is 17 J higher than the USE in the unirradiated condition. The residual shift, ΔT_{res}, is 24°C. The fracture toughness specimens were annealed at 454°C for 168 h. The residual shift of the reference transition temperature is 13°C (Figure 6.2).

Figures 6.3 and 6.4 present CVN and fracture toughness properties, respectively, of HSST plate 02 in the unirradiated, irradiated, and irradiated/annealed conditions. Annealing at 343°C for 168 h resulted in full recovery of the USE. The residual shift of the CVN transition temperature after annealing at 343°C is 35°C. Similar to the Midland weld, annealing at 454°C for 168 h resulted in "over-recovery" of the USE; the USE of the irradiated and annealed plate rose 24 J above the USE in the unirradiated condition. Regarding the transition temperature, almost full recovery was observed after annealing at 454°C/168 h, and the residual shift was only 6°C. The residual shifts of the fracture toughness, however, were 78 and 22°C after annealing at 343 and 454°C, respectively.[1] For both materials, full recovery of the CVN USE was observed even at the lower annealing temperature, although recovery of the transition temperature was far from complete at 343°C. One set of HSSI weld 73W specimens irradiated in capsule 10-5 was also annealed at 343°C for 1 week (see Figure 6.5). Low-temperature annealing resulted in partial recovery of the transition temperature but significant recovery of the USE.

At the annealing temperature of 454°C, over-recovery of the USE of the materials studied was observed. The definition of over-recovery is that the USE after annealing of irradiated material is greater than in the unirradiated level. Such behavior is consistent with annealing studies of HSSI weld 73W published in a previous report.[2] Based on results of that work and analysis of published data, it is shown that, as a rule, the USE is recovered faster

ORNL-DWG95-5914

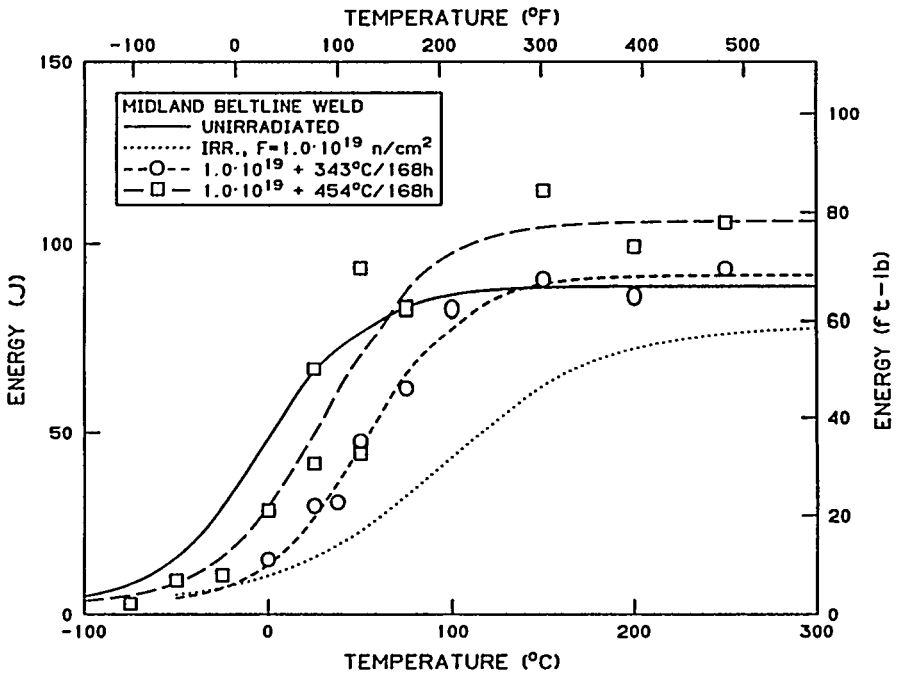

Figure 6.1. Charpy V-notch impact energy of the Midland beltline weld in the unirradiated, irradiated, and iradiated/annealed conditions.

ORNL-DWG95-5915

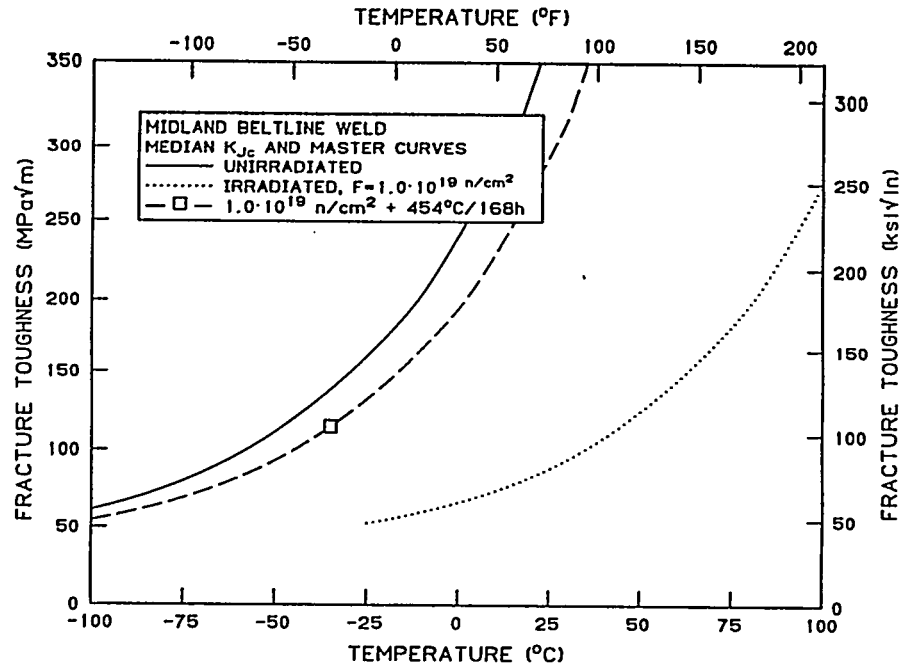

Figure 6.2. Fracture toughness properties of the Midland beltline weld in the unirradiated, irradiated, and irradiated/annealed conditions.

ORNL-DWG95-5916

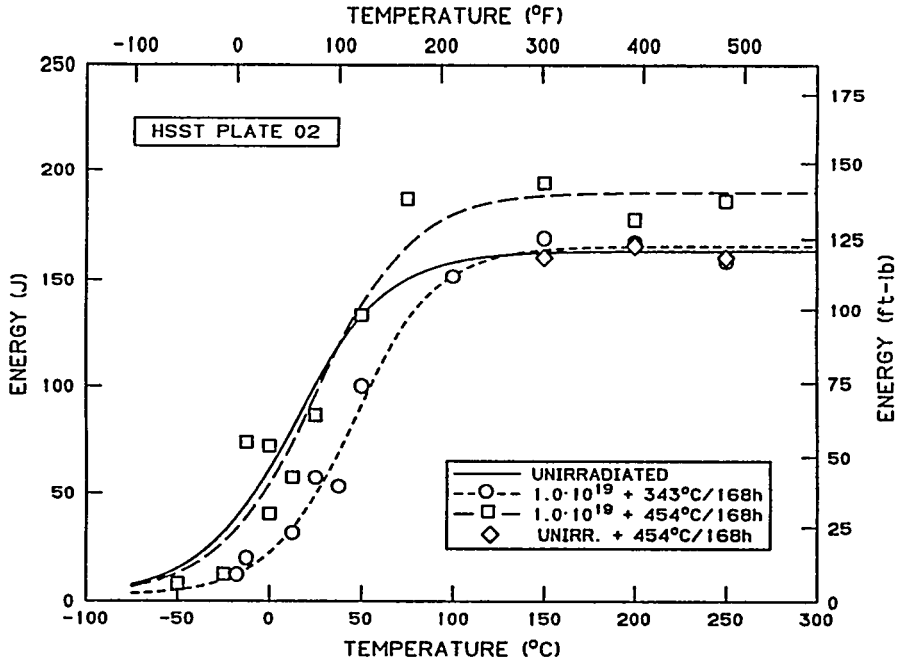

Figure 6.3 Charpy V-notch impact energy of HSST plate 02 in the unirradiated and irradiated/annealed conditions.

ORNL-DWG95-5917

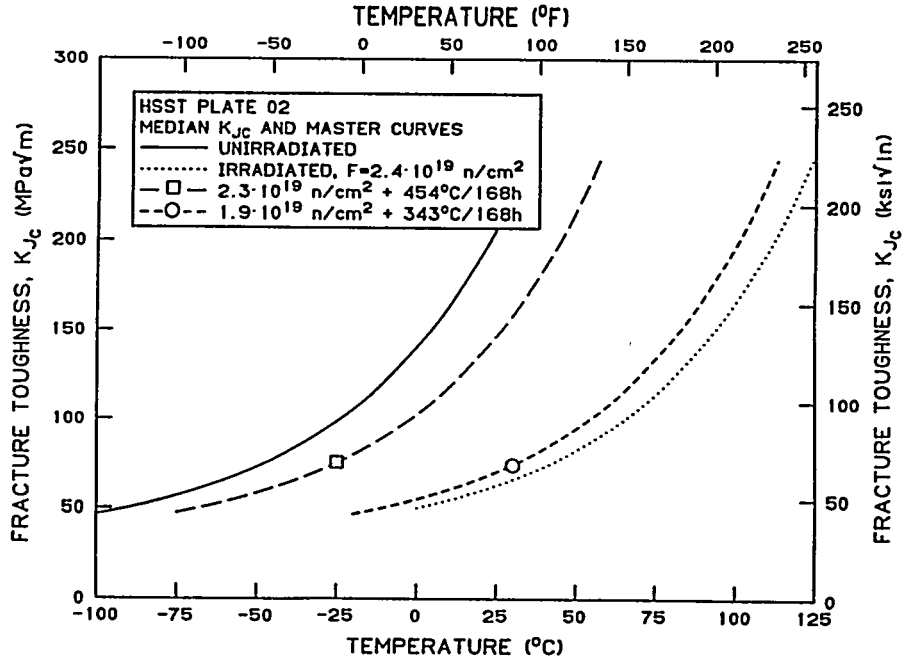

Figure 6.4. Fracture toughness properties of HSST plate 02 in the unirradiated, irradiated, and irradiated/annealed conditions.

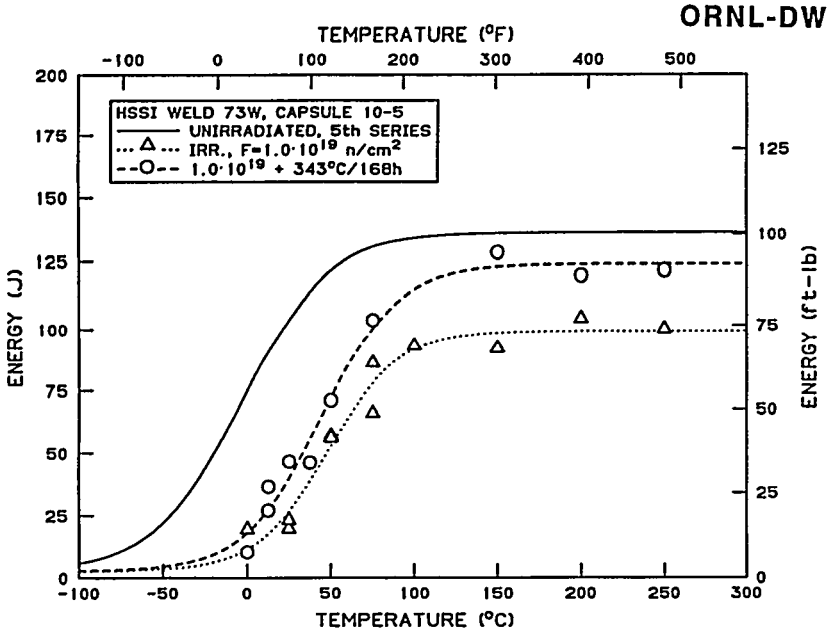

Figure 6.5. Charpy V-notch impact energy of HSSI weld 73W irradiated in capsule 10.5 in the unirradiated, irradiated, and irradiated/annealed conditions.

At the annealing temperature of 454°C, over-recovery of the USE of the materials studied was observed. The definition of over-recovery is that the USE after annealing of irradiated material is greater than in the unirradiated level. Such behavior is consistent with annealing studies of HSSI weld 73W published in a previous report.[2] Based on results of that work and analysis of published data, it is shown that, as a rule, the USE is recovered faster than the transition temperature. It is also shown that annealing of irradiated and unirradiated submerged-arc HSSI weld 73W at 454°C for 168 h resulted in the same increase of the USE compared with the unirradiated condition. The mechanisms and processes that contribute to recovery and over-recovery of the USE are not yet fully understood and thus may be different in irradiated and unirradiated materials. One notable exception to the over-recovery exhibited by most of the materials tested in this task is HSST plate 02. Limited data for the CVN USE for *unirradiated* plate 02 material aged at 454°C for 168 h did not show any over-recovery of the USE, whereas *irradiated* plate 02 material showed significant over-recovery (see Figure 6.3). Annealing at 454°C for 168 h was repeated on CVN specimens from the Midland nozzle course weld irradiated to 1.0×10^{19} neutrons/cm^2 (> 1 MeV) at the FNR (Figure 6.6). The USE of the irradiated and annealed nozzle course weld increased by 17 J above the unirradiated level. The more rapid and more extensive recovery of USE with annealing compared with CVN transition temperature suggests a different mechanism for degradation of these properties upon irradiation. The over-recovery of CVN USE makes annealing an attractive measure, especially for so-called low-USE welds. However, the real value of this advantage can be judged only after an extensive study of the behavior of materials after reirradiation. All materials and conditions studied will be reirradiated to measure the rate of reembrittlement.

6.3 Design, Fabrication, and Installation of New Irradiation Facilities (D. W. Heatherly, C. A. Baldwin, D. W. Sparks , and G. E. Giles, Jr.)

All design work for the IAR facilities was completed, and two facilities are in the process of being fabricated. Design work for the experimental capsules was completed, and one test temperature capsule is presently in the fabrication stage. A dosimeter test capsule that will be used to characterize all of the four planned IAR facilities has

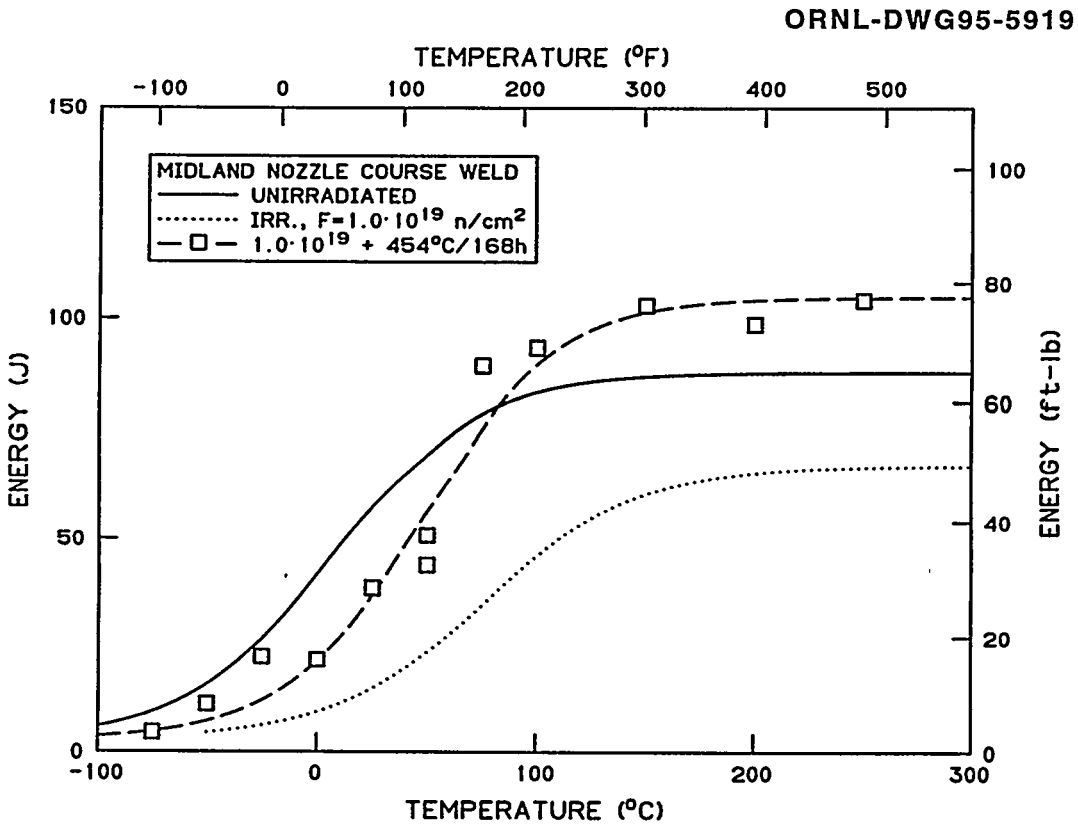

Figure 6.6. Charpy V-notch impact energy of Midland nozzle course weld irradiated in capsule 10.5 in the unirradiated, irradiated, and irradiated/annealed conditions.

been designed and is also in the fabrication stage. Irradiated and annealed specimens, presently stored in the ORNL hot cells, will be reirradiated in the HSSI IAR facilities. Loading irradiated specimens into the IAR facilities required designing a new reirradiation capsule that could be loaded with specimens in the FNR hot cell. This capsule, fabricated to house preirradiated specimens, had to be designed with a flexible section that would allow the entire capsule assembly to be transferred from the FNR hot cells to the reactor pool through a transfer tube between the reactor pool and the hot cell. The experiment is designed so that, after irradiation of the initial specimens, the capsule can be transferred to the FNR hot cells where the original specimens can be removed and replaced. The present plan calls for one reusable capsule to be used in about four reirradiations. In addition, using the same test capsule for all the irradiations minimizes the disposal of irradiated hardware after the tests are completed.

6.4 Data Acquisition and Control System (M.T. Hurst)

The DAC instrumentation for the first two IAR facilities is essentially complete and is awaiting completion of the IAR facilities and temperature test capsule for checkout and control algorithm development. The DAC has the capability to store data and control the proposed four IAR capsules. This system also has the capabilities to interface to the Santa Barbara capsules through the network for DAC. Figure 6.7 shows a schematic for this system. The present configuration allows DAC for 24 heater zones, 64 temperature inputs, 8 gas control loops, and 8 pressure and 2 vacuum control systems. The present system allows for Ethernet Transmission Control Protocol/Internet Protocol for networking. Figure 6.7 also shows future expansion to a total of four instrument cabinets; one main control cabinet, which contains the DAC hardware; two experimental auto/manual gas control interface cabinets; and one heater control cabinet. The Santa Barbara facility shows one cabinet for DAC and one combination gas and electric heater control auto/manual cabinet networked through the HSSI facility.

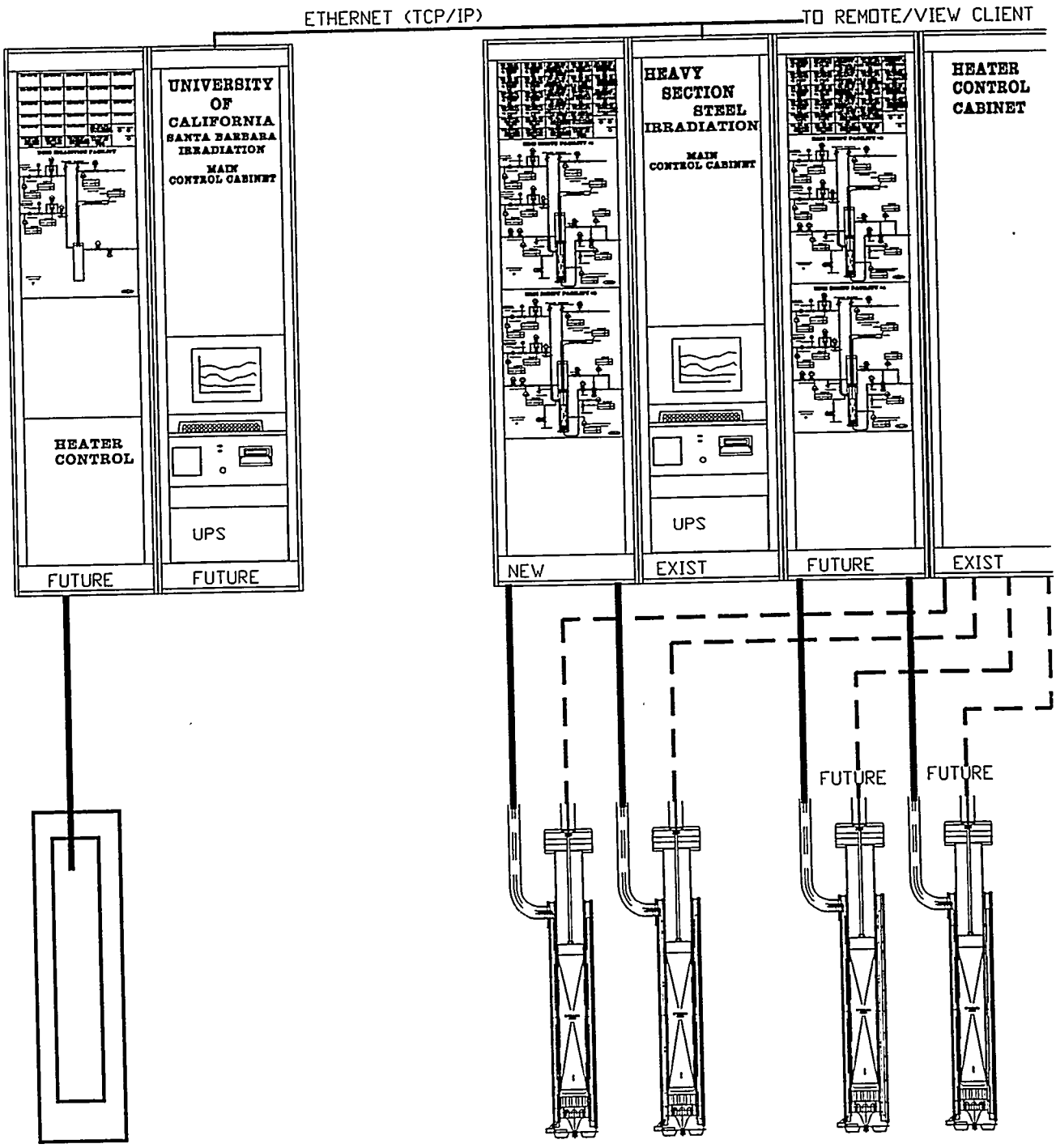

Figure 6.7. Schematic of the new irradiation, annealing, and reirradiation facilities.

The future expansion for the HSSI facility hardware for the second gas auto/manual cabinet and related input/output (I/O) hardware would need to be procured and fabricated identical to IAR control cabinets 1 and 2. The Santa Barbara facility would consist of procurement and fabrication of two cabinets with related hardware and I/O modules interfaced as a separate node through the HSSI software.

References

1. J. J. McGowan, R. K. Nanstad, and K. R. Thoms, Martin Marietta Energy Systems, Inc., Oak Ridge Natl. Lab., *Characterization of Irradiated Current-Practice Welds and A 533 Grade B Class 1 Plate for Nuclear Pressure Vessel Service*, USNRC Report NUREG/CR-4880, Vol. 1 (ORNL/TM-6484/V1), July 1988.*

2. S. K. Iskander et al., Martin Marietta Energy Systems, Inc., Oak Ridge Natl. Lab., "Annealing Effects in Low Upper Shelf Welds," in *Heavy-Section Steel Irradiation Program Semiannual Progress Report October 1993–March 1994*, USNRC Report NUREG/CR-5591, Vol. 5, No. 1 (ORNL/TM-11568/V5&N1), 1995.*

*Available for purchase from National Technical Information Service, Springfield, VA 22161.

7. Microstructural Analysis of Radiation Effects

R. E. Stoller, P. M. Rice, K. Farrell, and C. C. Goodwin

7.1 Analysis of Thermal Aging and Irradiation Effects in RPV Steels by Atom-Probe Field-Ion Microscopy - R. E. Stoller, P. M. Rice, M. K. Miller, and P. Pariege

Microstructural characterization was performed on long-term (~ 100,000-h) thermally aged and neutron-irradiated surveillance materials obtained from the Babcock & Wilcox Nuclear Technologies[1,2] and a high phosphorus weld from a Russian reactor. Although mechanical testing indicated that thermal aging did not cause any significant changes in the Charpy impact properties, it is important to determine if there are any changes in the composition of the matrix and if any ultrafine precipitates had formed due to the thermal component of service environment only. The characterization of the Russian weld was performed to determine if the behavior of a steel with a phosphorus level in excess of that typically found in Western steels changes, and to ascertain whether the results for formation of copper-enriched regions are specific to the narrow composition band of the Western steels or a more general phenomenon.

The ORNL APFIM is well suited to the microstructural characterization of neutron-irradiated RPV materials because of its near-atomic spatial resolution and ability to chemically analyze all elements[3]. In addition to detecting, chemically identifying, and determining the size, morphology, and approximate number density of ultrafine features, the atom probe is able to quantify the amount of each element remaining in solution in the matrix and the amount of solute segregated to grain or lath boundaries.

Long-term thermally aged surveillance materials

As-fabricated and long-term thermally aged [~ 100,000 h at 540°F (282°C)] weld A (0.28 wt % Cu) and weld B (0.30 wt % Cu), plate A (0.15 wt % Cu) and plate B (0.17 wt % Cu), and forging (0.02 wt % Cu) materials were investigated. The comparison between these materials permitted the investigation of potential thermal aging effects.

The atom-probe microstructural studies focused on the quantification of the matrix chemistry. These studies indicate that there was no significant microstructural evolution after a long-term thermal exposure. For example, the same copper level in the matrix was found before and after the long thermal aging treatment. The matrix copper content in both of the weld metals was significantly lower than the nominal bulk composition[2] (see Table 7.1). This copper depletion is due to copper precipitation during the postweld stress relief treatment. Only 70% of the nominal value is still in metastable solid solution. No copper depletion was found in the plates or the forging due to their lower initial copper content. These values are in agreement with the predicted copper solubility limit in iron.

Neutron-irradiated surveillance materials

Atom-probe investigations of the microstructure of neutron-irradiated weld A surveillance materials [6.6×10^{22} and 3.5×10^{23} n/m^2 (E > 1 MeV) at 560°F (294°C)] were also performed. A severe depletion of copper (which was more pronounced at the higher dose) was observed in the matrix; phosphorus was depleted as well. In addition, a high number density (~ 10^{23} and ~ 3×10^{23} m^{-3} after fluences of 6.6×10^{22} and 3.5×10^{23} n/m^2, respectively) of ultrafine (2- to 3- nm-diam) intragranular Cu-, P-, Ni-, Mn-, and Si-enriched clusters were observed. A representative composition profile through one of these features is shown in Figure 7.1. The size and composition of these copper-enriched clusters were similar at low and high fluences. Only their number density was found to increase with fluence.

Table 7.1. Comparison of the nominal bulk composition of weld B with that measured in the ferritic matrix of weld B in the as-received and thermally aged (103,000 h at 282°C) conditions

	Element composition (at. %)							
	Cu	Ni	Mn	Si	P	C	Mo	Cr
As-received	0.17	0.43	1.22	1.49	0.07	0.03	0.23	0.06
Thermally-aged	0.16	0.42	1.24	1.73	0.03	0.008	0.20	0.07
Nominal bulk	0.26	0.55	1.64	1.20	0.02	0.37	0.22	0.10

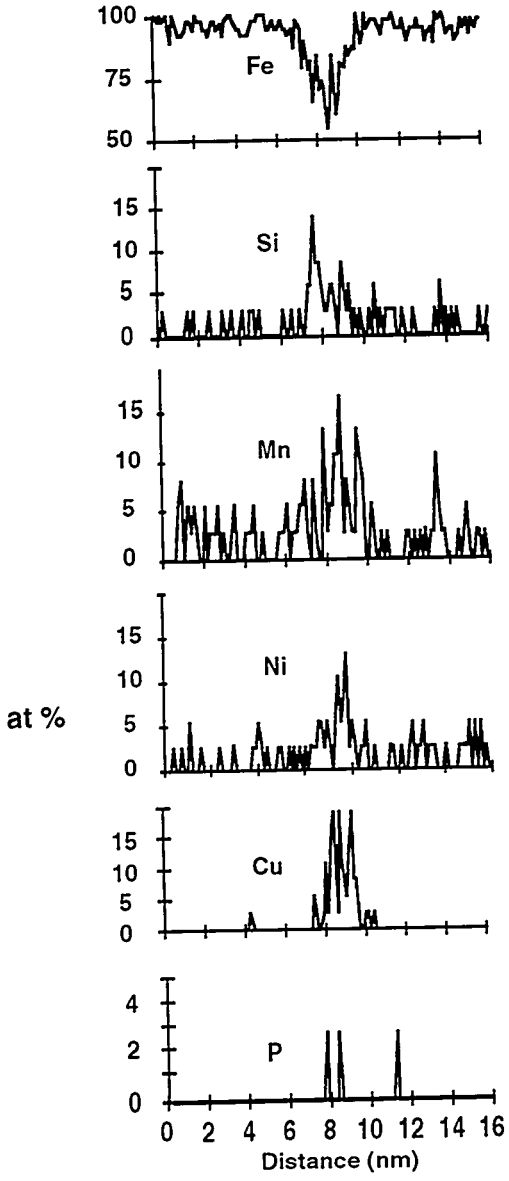

Figure 7.1. Composition profile through a copper-rich solute cluster in weld A irradiated to 3.5×10^{23} n/m.

This combination of materials and conditions permitted the investigation of long-term thermal aging as well as the neutron-induced effects. These APFIM comparisons of materials in all three conditions are consistent with the measured change in mechanical properties (transition temperature shift) for both aging conditions. Experiments on neutron-irradiated plate and forging materials are now in progress as well as studies on the effects of annealing treatments.

High phosphorus Russian pressure vessel steel

An atom-probe characterization of a Russian weld material that contained 0.14 wt % Cu and 0.035 wt % P in both the unirradiated condition and after neutron irradiations to fluences of 1×10^{23} and 1.15×10^{24} n/m^2 has been performed. Particular emphasis was placed on determining the distribution of copper and phosphorus in the alloy.

Atom-probe analysis revealed that ultrafine copper and phosphorus clusters were formed in both neutron-irradiated materials. The copper clusters were also enriched in manganese, silicon, and phosphorus, and phosphorus was detected at the vanadium carbonitride/matrix interface. The matrix showed a corresponding depletion in copper and phosphorus.

The phosphorus coverage at lath boundaries was determined from atom-probe data with the Gibbsian interfacial energy method. These results indicated that the phosphorus coverage at the boundaries in the control material was ~ 16% of a monolayer. This value is in reasonable agreement with the prediction obtained from the McLean model of equilibrium segregation of ~ 13% of a monolayer for this phosphorus content and the thermal history of the weld. These values are approximately a factor of three higher than those typically found in Western A533B steels since the phosphorus content was significantly higher in this Russian weld. It should also be noted that predictions from the McLean equilibrium model for postirradiation thermal annealing of these materials in the 400 to 475°C temperature range for 200 h indicate that the phosphorus coverage increases from the ~ 13% level up to ~ 40% of a monolayer. After neutron irradiation to a fluence of 1.15×10^{24} n/m^2, the phosphorus coverage had increased significantly, up to 60% of a monolayer, indicating that the neutron irradiation had accelerated the segregation process. The boundaries were also decorated with an ultrathin film of molybdenum carbonitride precipitates and were a site for heterogeneous precipitation of the 5- to 10-nm vanadium carbonitride precipitates.

7.2. Mechanical Property and Microstructural Examination of Aged and Ion-irradiated Materials

A topical report describing the TEM characterization of the nine model steels selected for use in the ion irradiation experiments was completed. The TEM observation verified that the alloys were appropriate for the irradiation experiments. The microstructures were typical of clean model alloys, with low dislocation densities, large grains, and a low density of precipitates and inclusions as a result of the solute impurities. The expected effects of intentional alloying or doping with Cu, Mn, Ti, C, and N were observed. For example, the addition of N and C led to a formation of a relatively high density of carbo-nitrides. The addition of Ti suppressed the formation of the larger carbo-nitrides; a fine dispersion of TiC was observed.

The model alloy from this set of nine that contains the greatest amount of copper, Fe-0.9 Cu, has been thermally aged to obtain hardening information on the copper precipitates that form. Initial TEM examination of these specimens indicates that the precipitates transform from body-centered cubic (bcc) to the faulted 9R (reference 4) structure when they reach a diameter of about 6 nm. The hardness change as a function of annealing time at 550°C is shown in Figure 7.2. A comparison of the copper precipitate distributions and nanohardness measurements indicates that visible precipitates (larger than 6 nm diam) can account for only a fraction of the hardness change measured. These precipitates can be imaged more easily since they have converted to the 9R structure and are not coherent with the bcc ferrite matrix. A typical precipitate size distribution is shown in Figure 7.3. Alternate techniques are being investigated to image the smaller, coherent bcc copper precipitates that should be present. For example, although a newly installed, electron-energy-filtering imaging system provides a chemical map showing the larger 9R or face-centered cubic precipitates, it has so far lacked sufficient stability to reveal the bcc precipitates. Further work with the new system is ongoing.

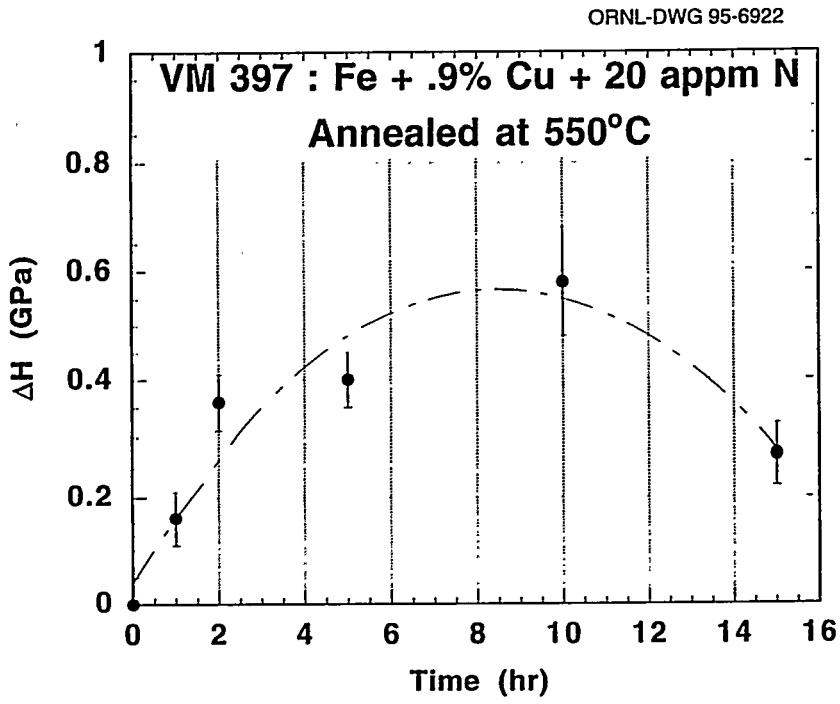

Figure 7.2. Hardness change observed in Fe-0.9 Cu after annealing at 550°C.

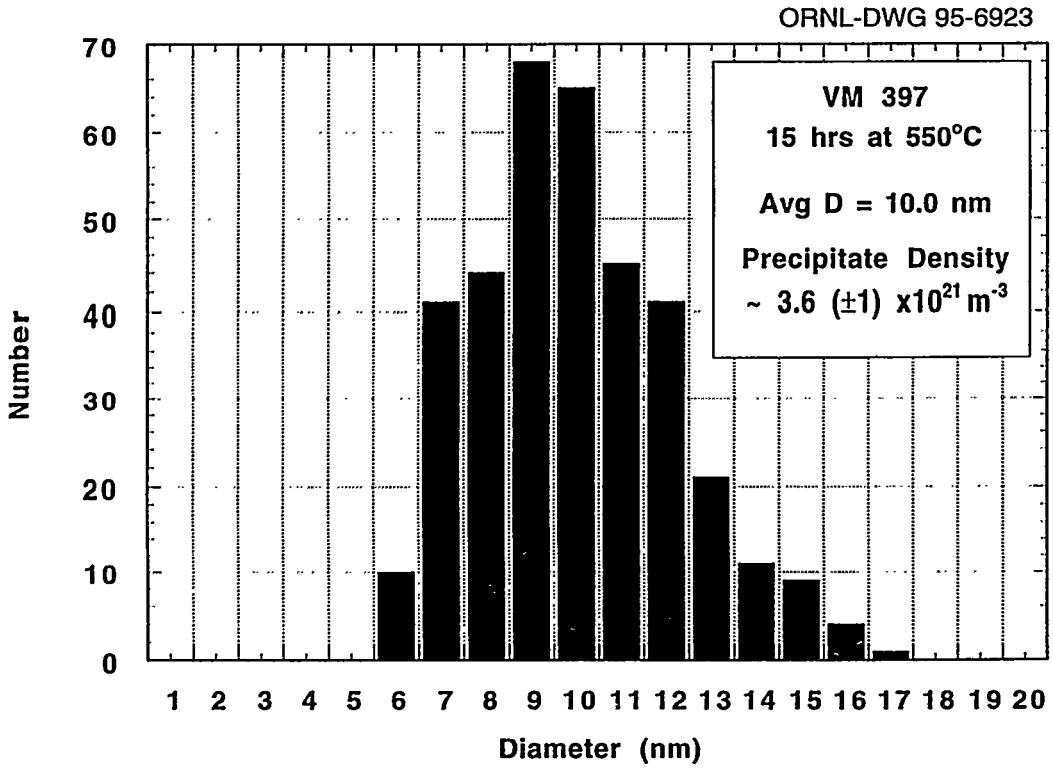

Figure 7.3. Size distribution of 9R copper precipitates observed in Fe-0.9 Cu after annealing at 550°C for 15 h.

The copper dependence of hardening in the low-nitrogen model alloys is shown in Figure 7.4. The TEM evaluation of these specimens indicates that the hardening is primarily due to a fine distribution of point defect clusters (PDCs). A measured PDC size distribution is shown in Figure 7.5. An evaluation of the PDC size distribution and the hardness change using the conventional Orowan dispersed barrier theory leads to an effective PDC barrier strength of 0.2. This is consistent with the PDCs being small dislocation loops. The data from the annealing and ion irradiation experiments are being used to update the kinetic models that are being developed as part of this task.

7.3 Irradiation Experiment Investigating Spectral Effects

The final irradiation in the series of experiments that were initiated to investigate flux rate and spectral effects at the low temperatures relevant to RPV support structures was completed. This irradiation was conducted using the High Flux Beam Reactor (HFBR) at Brookhaven National Laboratory and focused on determining the influence of a very high ratio of thermal to fast neutrons. The heavy water moderator in the HFBR yields a thermal-to-fast flux ratio of 368 in one of the positions used. Several alloys were irradiated in the form of SS-3 minitensiles. This experiment included a set of samples that were irradiated for the University of California, Santa Barbara (UCSB). Specimen capsules have been shipped from the HFBR to ORNL, and the UCSB specimens were sent to Santa Barbara. Specimen testing will be conducted during the next reporting period.

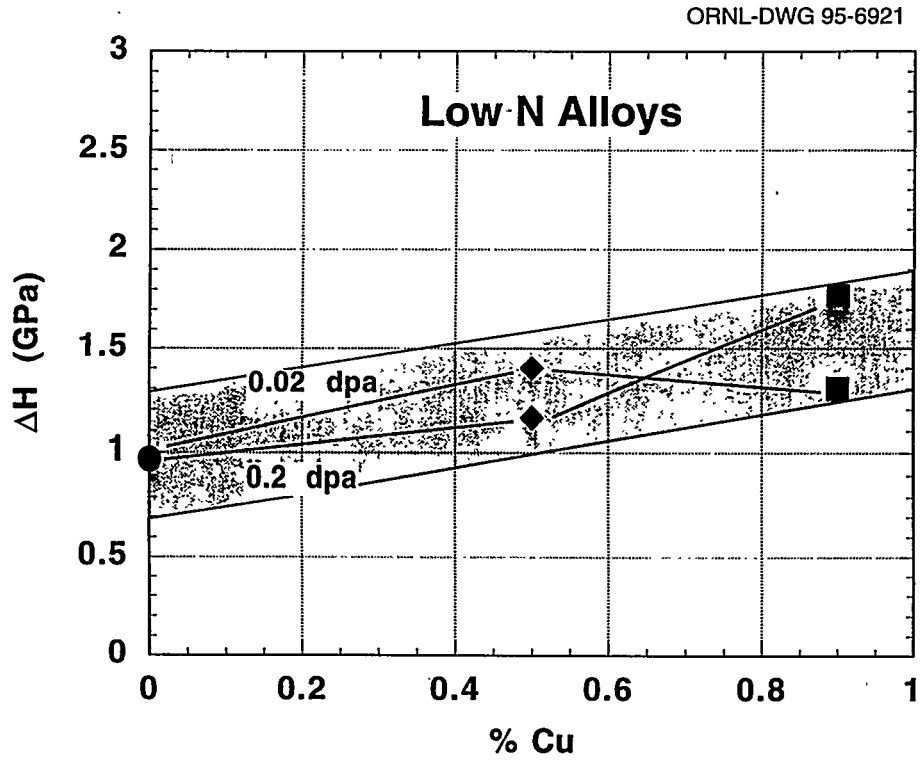

Figure 7.4 **Hardness change observed in Fe, Fe-0.5 Cu, and Fe-0.9 Cu after ion irradiation at 300°C.**

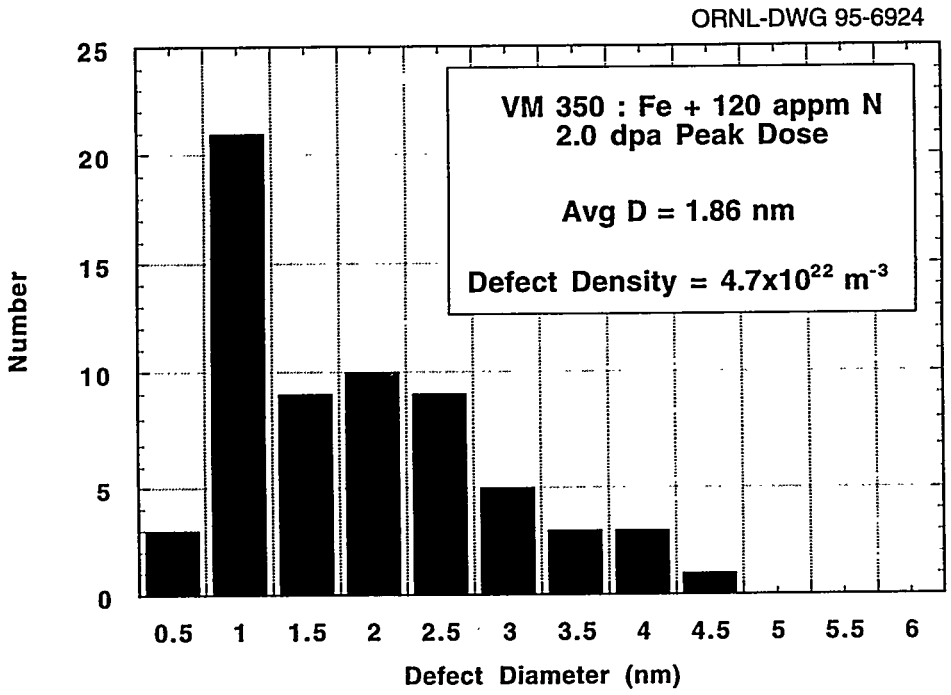

Figure 7.5. Size distribution of point defect clusters observed in Fe-120 appm N after ion irradiation at 300°C.

7.4 Modeling and Data Analysis

As part of the ongoing evaluation of commercial reactor embrittlement database and *Regulatory Guide 1.99*, surveillance data from French pressurized-water reactors (PWRs) have been collected from the published literature and formatted for computerized analysis. This data set currently includes chemical compositions, unirradiated properties, and CVN shifts for 70 plate irradiation conditions, 52 weld irradiation conditions, and 49 HAZ irradiation conditions. Both unirradiated and irradiated tensile properties are also available for most of the conditions. An initial comparison of the *Regulatory Guide 1.99, Rev. 2*, predictions and the measured shifts indicates that the overall behavior is consistent with the American data in the power-reactor embrittlement data (PR-EDB). The mean residuals and standard deviations are similar for both data sets if the Chooz reactor data are excluded. The vessel in this latter reactor operated at about 265°C, or 20°C colder than most PWRs.

A set of data from the PR-EDB has been selected for a new comparison of fast fluence and displacements per atom (dpa) as a correlation parameter. These data were selected from a single vendor who has recently completed a reanalysis of capsule fluences and recalculated dpa values in a self-consistent manner. In order to make this comparison, the data are being fit using two fluence/dpa models. The first is a *Regulatory Guide 1.99*-type model incorporating some chemical effects, and the second is a more simple model, depending only on the total exposure. A copy of the SPECTER computer code[5] has been obtained from Dr. L. R. Greenwood at the Battelle Pacific Northwest Laboratories for use in computing effective, spectrum-averaged dpa cross sections as part of this work and in performing a more detailed comparison of PWR and boiling-water reactor (BWR) neutron energy spectra.

References

1. A. L. Lowe, Jr., "Thermal Aging Capsule Results from Oconee Nuclear Station-Unit 1," pp. 146-54 in *Radiation Embrittlement and Surveillance of Nuclear Reactor Pressure Vessels, ASTM STP 819*, ed. L. E. Steele, American Society for Testing and Materials, Philadelphia, 983.*

2. M. J. DeVan, A. L. Lowe, Jr., and C. S. Wade, "Evaluation of Thermal Aged Plants, Forgings and Submerged Arc Weld Metals," pp. 268-82 in *Effects of Radiation on Materials, ASTM STP 1175*, ed. A. S. Kumar, D. S. Gelles, R. K. Nanstad, and E. A. Little, American Society for Testing and Materials, Philadelphia, 1993.†

3. M. K. Miller, M. G. Hetherington, and M. G. Burke., *Metall. Trans.* **20A**, 2651-61 (1989).†

4. P. J. Othen, M. L. Jenkins, G. D. W. Smith, and W. J. Phythian, *Philos. Mag. Let.* **64**, 383-91 (1991).*

5. L. R. Greenwood and R. K. Smither, "*SPECTER: Neutron Damage Calculations for Materials Irradiations*," ANL/FPP/TM-197, Argonne National Laboratory, Chicago, Illinois, January 1985.†

*Available for purchase from National Technical Information Service, Springfield, VA 22161.
†Available in public libraries.

8. In-Service Irradiated And Aged Material Evaluations

F. M. Haggag, R. K. Nanstad, and D. J. Alexander

The objective of this task is to provide a direct assessment of actual material properties in irradiated components of nuclear reactors, including the effects of irradiation and aging. Four activities are currently in progress: (1) establishing a machining capability for contaminated or activated materials by completing procurement and installation of a computer-based milling machine in a hot cell; (2) machining and testing specimens from cladding materials removed from the Gundremmingen reactor to establish their fracture properties; (3) preparing an interpretive report on the effects of neutron irradiation on cladding; and (4) continuing the evaluation of long-term aging of austenitic structural stainless steel weld metal by metallurgically examining and testing specimens aged at 288 and 343°C and reporting the results, as well as by continuing the aging of the stainless steel cladding toward a total time of 50,000 h.

8.1 Installation of Remotely Operated Machining Center

Enclosure and floor designs and drawings were made for hot cell installation of the computer numerically controlled (CNC) machining center (model VMC-100). Also, drawings were made for installing a new saw for use inside the hot cell (to slice irradiated materials into smaller pieces suitable for specimen fabrication using the small CNC machine).

8.2 Thermal Aging of Stainless Steel Weld Overlay Cladding

Tensile, CVN, and fracture toughness testing of three-wire stainless steel cladding, thermally aged for 20,000 h at 288 and at 343°C, was completed and a draft report was prepared. The test results show that the effects of thermal aging at both temperatures were very small and similar to those reported earlier for 1605-h aging at 288°C. Hence, aging of additional three-wire cladding at 288°C for 50,000 h (completion expected in July 1996) and greater is continuing to better quantify the effects of long-term thermal aging.

8.3 Thermal Aging of Type 308 Stainless Steel Welds

Tensile specimens of type 308 stainless steel weldments that were aged at 343°C for 50,000 h have been tested. The results show that aging has little effect on the tensile properties, in agreement with prior results for material aged up to 20,000 h. Fractographic studies of the tensile and Charpy specimens will be conducted.

9. JPDR Vessel Steel Examination

W. R. Corwin, B. L. Broadhead, and M. A. Sokolov

There is a need to validate the results of irradiation effects research by the examination of material taken directly from the wall of a pressure vessel which has been irradiated during normal service. This task has been included with the HSSI Program to provide just such an evaluation of material from the wall of the pressure vessel from the JPDR.

The JPDR was a small BWR that began operation in 1963. It operated until 1976, accumulating ~17,000 h of operation, of which a little over 14,000 h were with the original 45-MWTh core, and the remaining fraction, late in life, with an upgraded 90-MWTh core. The pressure vessel of the JPDR, fabricated from A 302, grade B, modified steel with an internal weld overlay cladding of 304 stainless steel, is approximately 2 m ID and 73 mm thick. It was fabricated from two shell halves joined by longitudinal seam welds located 180° from each other. The rolling direction of the shell plates is parallel to the axis of the vessel. It operated at 273°C and reached a maximum fluence of about 2.3×10^{18} n/cm^2 (> 1 MeV). The impurity contents in the base metal are 0.10 to 0.11% Cu and 0.010 to 0.017% P with a nickel content of 0.63 to 0.65%. Impurity contents of the weld metal are 0.11 to 0.14% Cu and 0.025 to 0.039% P with a nickel content of 0.59%.

The current status of the JPDR pressure vessel is that it has been cut into pieces, roughly 800 × 800 mm × the original local wall thickness. Full-thickness trepans have been cut from one of the sections originally located at the core beltline and from one of the sections near the upper flange, well away from the beltline. Eight beltline trepans were removed containing the longitudinal fabrication weld as were eight beltline trepans located completely within the base metal. Nine remotely located trepans were taken containing the longitudinal fabrication weld as were 14 containing only base metal. JAERI has shipped the irradiated material from the wall of the JPDR that will be examined at ORNL, where it was subsequently received, and moved into the hot cells where it is to be machined and examined. The material received at ORNL consists of 16 full-thickness trepans, each approximately 87 mm in diameter. The trepans contain four types of material: weld metal and base metal, each in both the irradiated condition (from the beltline) and in nominally, thermally aged-only condition (from the upper flange). ORNL received four trepans of each material. JAERI has placed all the remaining vessel material in a hot warehouse on-site for long-term storage and currently has no plans to do anything else with it.

The objectives of the JAERI JPDR pressure vessel investigations are to obtain materials property information on the pressure vessel steel actually exposed to in-service irradiation conditions and to help validate the methodology for aging evaluation and life prediction of RPVs. The Japanese research associated with the evaluation of irradiation effects is composed of three parts: examination of material from the JPDR vessel in conjunction with a reevaluation of its exposure conditions, new test reactor irradiations of archival and similar materials, and reevaluation of data from irradiation surveillance and related programs. The focus of the research to be performed by ORNL on the JPDR material is the determination of irradiation-induced damage through the thickness of the vessel in the beltline region and its comparison with the properties and microstructural evaluations of the same material following short, high-rate irradiations or with thermal damage only. This will be done by fabricating fracture and microstructural specimens from the trepans taken from the beltline and from the region remote from the beltline. Parallel determinations of exposure will be made by dosimetry measurements taken on the vessel material itself and by supporting neutron transport calculations.

During this reporting period, detailed plans were implemented and work was virtually concluded to evaluate the existing neutron dosimetry and transport calculations which have been performed for the JPDR by the Japanese, as well as to perform similar transport calculations at ORNL. The ORNL transport calculations included the

concrete in the biological shield as well as the pressure vessel. This allowed participation in the International Atomic Energy Agency (IAEA) exercise on concrete activation for decommissioning, as well as the original program aims to determine flux and fluence levels within the vessel itself.

Neutron transport studies were performed to quantify the neutron fluence parameters for correlation with pressure vessel metallurgical property examinations. Simple one-dimensional and more detailed two-dimensional neutron transport analyses quantified both the neutron fluence parameters (fluence greater than 0.1 and 1 MeV) as well as activation in the pressure vessel steel and biological shield concrete materials. The activation results were used in an IAEA sponsored benchmark study of fission reactor decommissioning issues. Activation measurements in the JPDR reactor served as benchmark data which were analyzed by participants in the study group. The neutron transport analyses served the dual role of satisfying both objectives, while lending credence to the neutron fluence parameters for which direct measurements are not available. Material property studies ongoing for the biological shield concrete are also aided by these results since neutron fluence parameters are also obtained for the concrete.

Initial activation results for the IAEA benchmark problem are shown in Figures 9.1 and 9.2 for the JPDR pressure vessel and biological shield. These results show generally good agreement with the measured cobalt activation in the JPDR pressure vessel, while the JPDR biological results show up to a factor of ten overprediction of the measured data for the biological shield. Efforts are currently under way to investigate suspected causes of this discrepancy in the biological shield. Final results using corrected models will be obtained prior to publication of complete study results.

ORNL-DWG95-5922

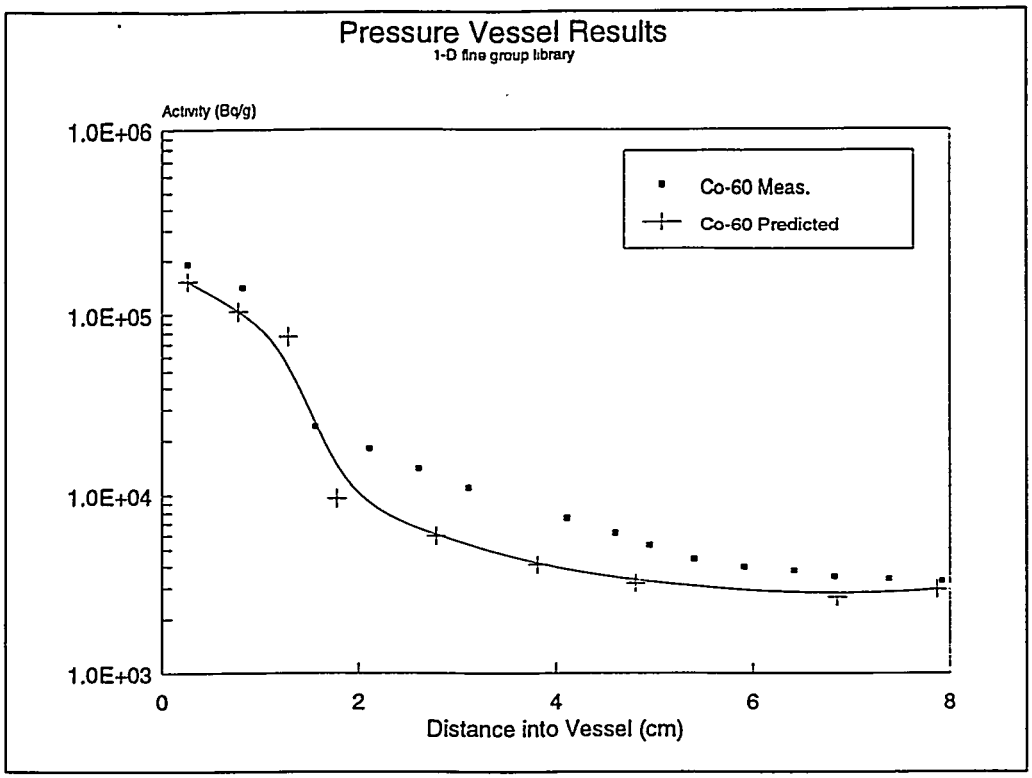

Figure 9.1. One-dimensional fine-group ^{60}Co activation results in JPDR pressure vessel.

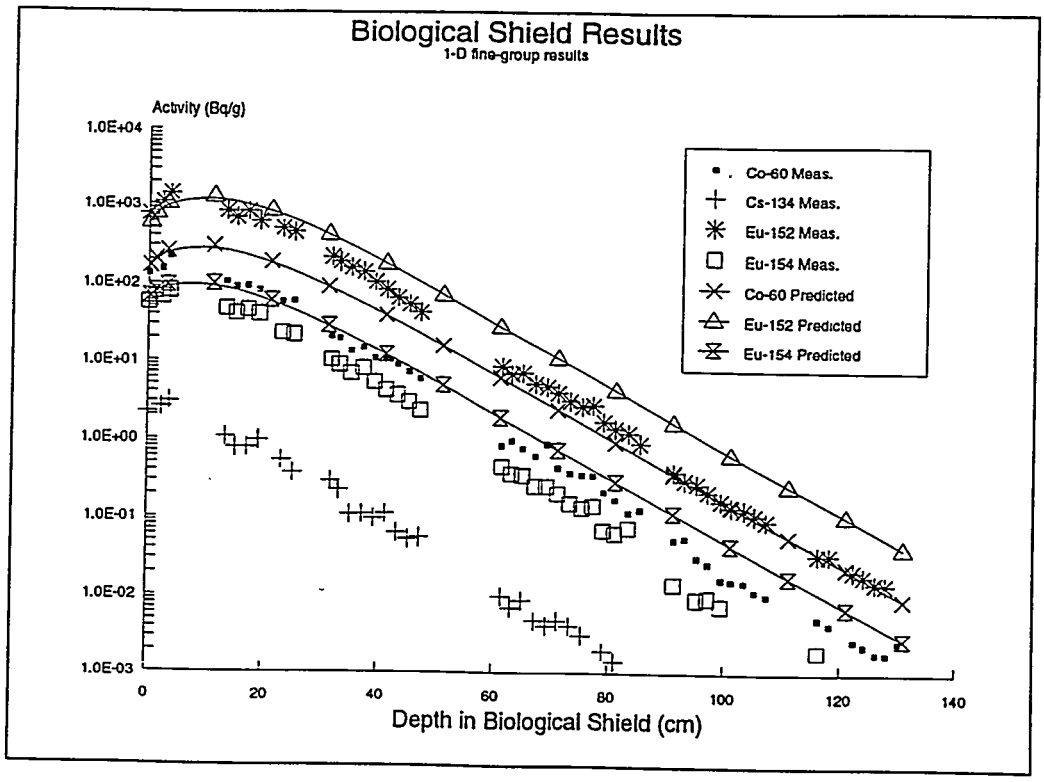

Figure 9.2. One-dimensional fine-group activation results in the JPDR biological shield.

10. Fracture Toughness Curve Shift Method

R. K. Nanstad, M. A. Sokolov, and D. E. McCabe

The purpose of this task is to examine the technical basis for the currently accepted methods for shifting fracture toughness curves to account for irradiation damage, and to work through national codes and standards bodies to revise those methods, if a change is warranted. Specific activities under this task include: (1) collection and statistical analysis of pertinent fracture toughness data to assess the shift and potential change in shape of the fracture toughness curves due to neutron irradiation, thermal aging, or both; (2) evaluation of methods for indexing fracture toughness curves to values that can be deduced from material surveillance programs required under the *Code of Federal Regulations* (10CFR50), Appendix H; (3) participation in the pertinent ASME Section XI, ASTM E-8, and ASTM E-10 committees to facilitate obtaining data and disseminating the results of the research; (4) interaction with other researchers in the national and international technical community addressing similar problems; and (5) frequent interaction, telephone conversations, and detailed technical meetings with the NRC staff to ensure that the results of the research and proposed changes to the accepted methods for shifting the fracture toughness curves reflect staff assessments of the regulatory issues.

During this reporting period, data from all the relevant HSSI Programs were acquired and stored in a database and evaluated. The results from that evaluation have been prepared in a draft letter report and are summarized here. A method employing Weibull statistics was applied to analyze fracture toughness properties of unirradiated and irradiated pressure vessel steels. Application of the concept of a master curve for irradiated materials was examined and used to measure shifts of fracture toughness transition curves. It was shown that the maximum likelihood approach gave good estimations of the reference temperature, T_o, determined by rank method and could be used for analyzing of data sets where application of the rank method did not prove to be feasible. It was shown that, on average, the fracture toughness shifts generally exceeded the Charpy 41-J shifts; a linear least-squares fit to the data set yielded a slope of 1.15. The observed dissimilarity was analyzed by taking into account differences in effects of irradiation on Charpy impact and fracture toughness properties. Based on these comparisons, a procedure to adjust Charpy 41-J shifts for achieving a more reliable correlation with the fracture toughness shifts was evaluated. An adjustment consists of multiplying the 41-J energy level by the ratio of unirradiated to irradiated Charpy upper shelves to determine an irradiated transition temperature, and then subtracting the unirradiated transition temperature determined at 41 J. For LUS welds, however, an unirradiated level of 20 J (15 ft-lb) was used for the corresponding adjustment for irradiated material.

Tables 10.1 and 10.2 provide the identification, chemical compositions, and some fabrication details of the HSSI Program materials evaluated. Figure 10.1 graphically demonstrates the excellent comparison of the maximum likelihood and rank methods for determination of the reference fracture toughness transition temperature, T_o. Figure 10.2 provides a plot which compares the irradiation-induced shifts of the reference fracture toughness and Charpy 41-J transition temperatures. A linear fit to the data shows that, on average, the fracture toughness shifts exceed the Charpy shifts by about 15%. This result is dominated by the data with shifts greater than about 30°C. Results obtained from the adjustment procedures mentioned above are included in the letter report. All these procedures are still under evaluation and will be evaluated with the larger database which is being assembled.

Table 10.1. Chemical compositions of the materials studied in the HSSI Program

Material	Average composition (wt %)									
	C	Mn	P	S	Si	Cr	Ni	Mo	Cu	V
Plate 02	0.23	1.55	0.009	0.014	0.20	0.04	0.67	0.53	0.14	0.003
Weld 68W	0.15	1.38	0.008	0.009	0.16	0.04	0.13	0.60	0.04	0.007
Weld 69W	0.14	1.19	0.010	0.009	0.19	0.09	0.10	0.54	0.12	0.005
Weld 70W	0.10	1.48	0.011	0.011	0.44	0.13	0.63	0.47	0.056	0.004
Weld 71W	0.12	1.58	0.011	0.011	0.54	0.12	0.63	0.45	0.046	0.005
Weld 72W	0.09	1.60	0.006	0.006	0.44	0.27	0.60	0.58	0.23	0.003
Weld 73W	0.10	1.56	0.005	0.005	0.45	0.25	0.60	0.58	0.31	0.003
WF-70	0.08	1.61	0.017	0.007	0.62	0.11	0.57	0.41	0.26	0.004

Table 10.2. Postweld heat treatment summary

Material	Thickness (m)	Linde flux	Postweld heat treatment	
			Temperature (°C)	Time (h)
Plate 02	0.305		621[a]	40[a]
68W	0.178	0091	621	25
69W	0.300	0091	621	25
70W	0.175	0124	607	48
71W	0.175	80	607	48
72W	0.218	0124	607	40
73W	0.218	0124	607	40
WF-70	0.216	80	607	22

[a]Stress-relief heat treatment.

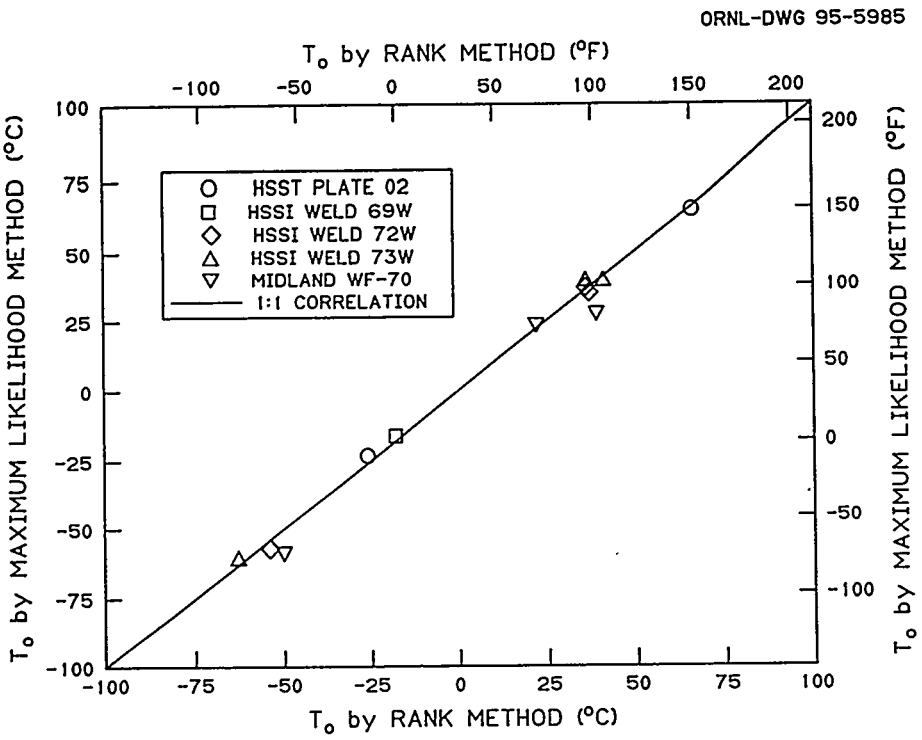

Fig. 10.1. Comparison of the reference fracture toughness transition temperature, T_o, determined by maximum likelihood and rank methods.

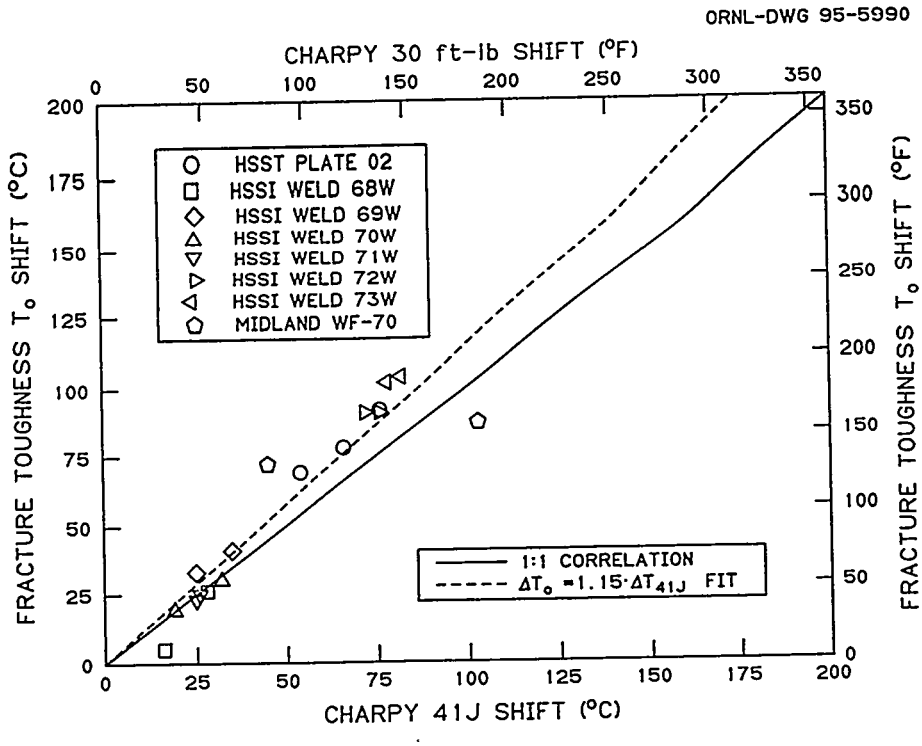

Fig. 10.2. Comparison of fracture toughness, T_o, and Charpy 41-J transition temperature shifts.

11. Special Technical Assistance

D. J. Alexander, R. K. Nanstad, and M. A. Sokolov

The purpose of this task is to perform various special analytical and experimental investigations to support the NRC in resolving regulatory research issues related to irradiation effects on materials. This task currently addresses two major areas: (1) providing technical expertise and assistance in the review of national codes and standards and (2) experimental evaluations of test specimens and practices and material properties.

11.1 Notched Round Tensile Bar Testing

SRI has completed their subcontract for initial testing of notched round bar specimens fabricated from weld 72W material. A final report has been written describing the test methods and results. The report will be issued as a NUREG (ORNL/TM) report.

Round tensile bars,16 mm in diameter, were taken transverse to the weld metal with their notch centered in the weld metal. The specimens were precracked in rotating four-point bending by loading them in a fixture on a lathe and applying a fixed displacement load. Crack extension was monitored by periodically removing the specimen and measuring the compliance in tension. This technique produced uniform annular precracks with very low eccentricity.

The specimens were tested over a range of temperatures from –150 to 50°C. Two extensometers mounted 90° from each other measured the displacement. This was corrected by subtracting the calculated displacement for an uncracked specimen. The area under the load-displacement curve was used to calculate the J-integral. The crack length was measured from the fracture surface after completion of the test.

Interrupted tests, acoustic emission examination, and fractographic examination of the broken specimens all indicated that crack extension began at or very near to maximum load. This was thus used as a convenient point for calculation of the J-integral at crack initiation. J-integral values were also calculated at final failure.

The results were compared to tests conducted at ORNL of 1T compact specimens from an essentially identical weld. The ORNL data were calculated at final fracture of the specimen, rather than at crack initiation. The comparison of the data is shown in Figure 11.1. The notched round bar results agree well with the 1T compact data in the middle of the transition regime. The notched bar data tend to show higher toughnesses than the 1T specimens at lower test temperatures. This is an unexpected result. Suggested reasons for the difference are: (1) possible inaccuracies in the J-integral formula, (2) differences in constraint between the two specimen types, (3) statistical size effects, and (4) possible differences between the two welds.

The broken specimens will be returned to ORNL. SRI has offered suggestions for further research on this topic.

11.2 Initial Evaluation of Subsize CVN Testing

A draft report describing the testing of subsize Charpy specimens has been written and is undergoing internal review. A new approach to normalizing data from subsize specimens was developed. This method gives excellent agreement with the data from full-size specimens for materials that have USE levels less than about 200 J.

Four types of RPV steels were selected for this study. Different heat treatments were used to provide ten material variants, with USEs of the full-sized specimens varying from 73 to 330 J, the transition temperatures from –46 to 58°C, and the yield strengths from 410 to 940 MPa. Five designs of subsize specimens were chosen for the present study.

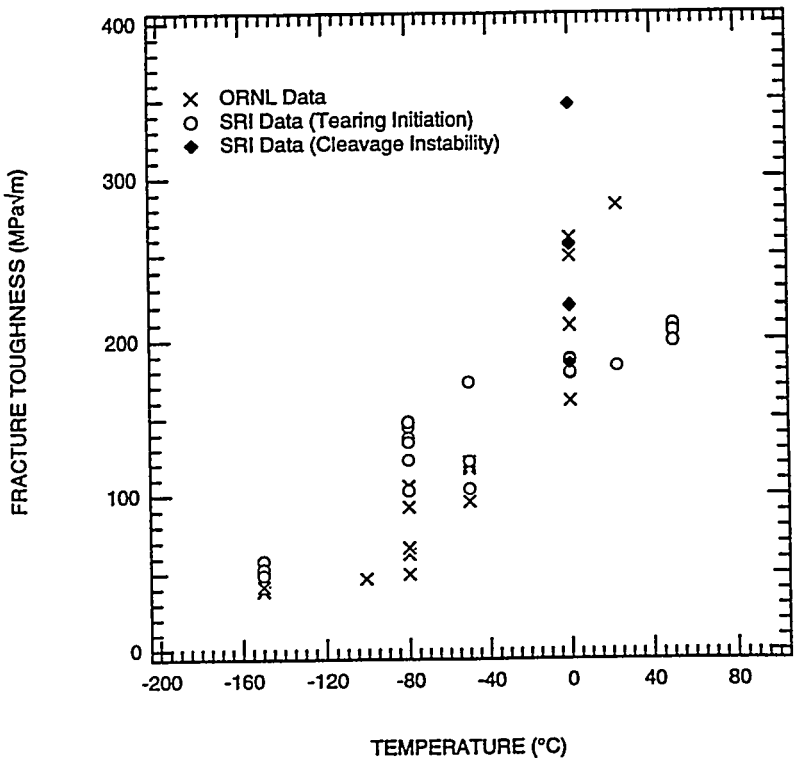

Figure 11.1 A comparison of the data from the notched round bar tests conducted by SRI with data from 1T compact specimens tested at ORNL.

For all types of subsize specimens, a linear dependence between the USE of full-size and subsize specimens was observed except for two materials that had USE from full-size specimens higher than 200 J. Specimens of materials with high-USE levels showed considerable plastic deformation at the anvil contact points caused by the specimen "wrapping around" the tup and squeezing through the anvils. This energy is significant but is not associated with the fracture process. Additional study is needed to analyze these data. For this study, analyses of data were limited to materials with USE levels less than 200 J for full-size specimens.

The normalization procedure of the data from subsize specimens involved two steps: a transformation of the energy values, followed by a temperature shift. The energy was divided into brittle and ductile components, based on the fracture surface appearance or the amount of rapid load drop from the voltage-time trace from the instrumented tup. The low-energy cleavage fracture was scaled by the ratio of the notched cross-sectional area of the full-size to the subsize specimen. The high-energy ductile fracture portion was scaled by an empirically determined value for the ratio of the USE of full-size to subsize specimens, unique for each type of subsize specimen. The scaled energy value was then given a new temperature value by adding a correction factor determined from:

$$DBTT_{full\ size} = DBTT_{subsize} + M \qquad (11.1)$$

where $DBTT_{full\ size}$ and $DBTT_{subsize}$ are transition temperatures for the full-size and the energy- corrected subsize specimen data, respectively, and M is a (constant) shift of the DBTT due to specimen size. Different specimen types will have different M values.

An example of the result of the normalization process is shown in Figure 11.2, which compares the data from four different types of subsize specimens with the mean value curve fit and 95% confidence intervals from a large set of data from full-size specimens. The normalization process gives excellent agreement between the corrected subsize data and the data from the full-size specimens.

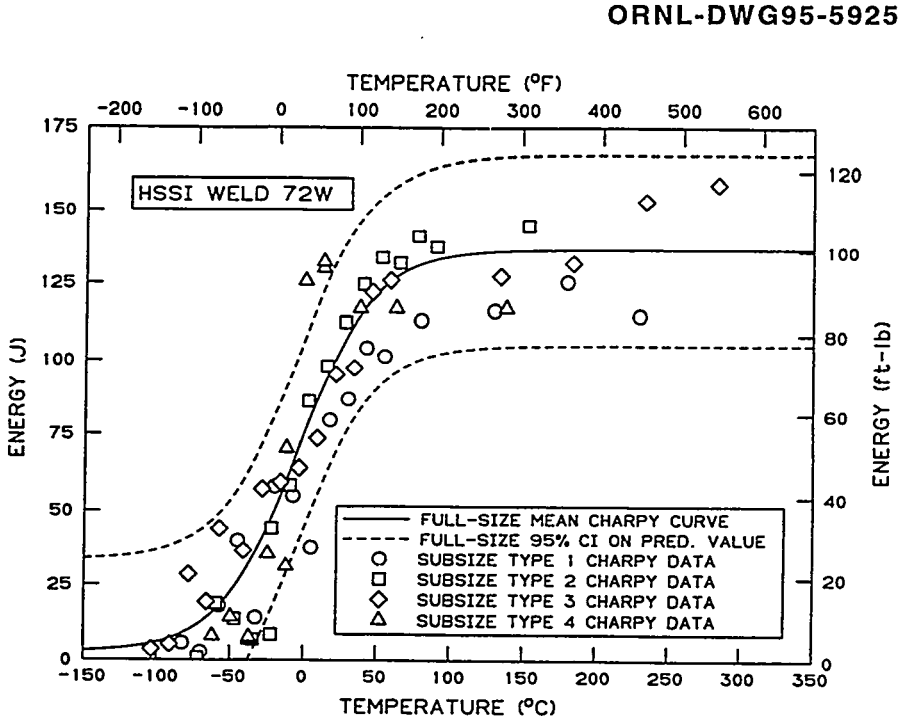

Figure 11.2. Comparison of Charpy curve for full-size specimens of HSST Weld 72W with data from subsize specimens normalized by the proposed procedure.

11.3 Reconstituted Round Robin

All of the reconstituted specimens have been tested. The results have been tabulated and transmitted to ASTM for their analysis and reporting.

11.4 Preliminary Review of Data Regarding Chemical Composition and Thermal Embrittlement of Reactor Vessel Steels

As a result of observations from recent studies with welds removed from retired steam generators of the Palisades Nuclear Plant (PNP), the NRC requested ORNL and other NRC contractors to prepare a preliminary review of thermal aging of RPV steels under nominal reactor operating conditions. This letter report, *Preliminary Review of Data Regarding Chemical Composition and Thermal Embrittlement of Reactor Vessel Steels*, by R. K. Nanstad, D. J. Alexander, W. R. Corwin, E. D. Eason, G. R. Odette, R. E. Stoller, and J. A. Wang (ORNL/NRC/LTR-95/1, January 1995), included discussions on (1) data from the literature regarding relatively low-temperature thermal embrittlement of RPV steels, (2) relevant data from the PR-EDB, (3) potential mechanisms of thermal embrittlement in low-alloy steels, and (4) the mechanical property and chemical composition data reported by Consumers Power Company (CPCO) for the steam generator welds and the database for welds fabricated with weld wire W5214.

The review of data from the literature concentrated on the shift in ductile-to-brittle transition temperature (DBTT) as a consequence of aging time for base metals, HAZ materials, and weld metals. For base metals typically used in fabrication of U.S.-type RPVs, the majority of data indicates little effect of aging at temperatures in the 500 to 600°F range, even for times as great as 100,000 h. Less data are available for HAZs of welds, but similar statements apply. It is noted, however, that the longest times studied systematically are 20,000 h. There are even fewer data available for weld metals. Again, most of the data suggests no substantial thermal embrittlement for typical weld metals in the temperature range of interest for up to 100,000 h. However, there are observations of thermal embrittlement in these steels in the temperature range of interest. There are uncertainties associated with some of those observations, but the potential for thermal embrittlement for times up to 30 to 40 years cannot be dismissed based on the data available. The observations for commercial steels are generally consistent with the discussion of thermal embrittlement mechanisms for the reported ranges of temperature and time. It is notable, however, that none of the reported data in the literature represents steels with the combination of high copper and high nickel such as that in the steam generator weld. There are indications from other studies regarding the synergistic effects of copper and nickel, as well as nickel and phosphorus, that do not allow us to assume that the observations from the literature are necessarily directly indicative of the entire range of materials of interest in U.S. RPVs.

A review of the PR-EDB was undertaken to examine the surveillance data for evidence of possible effects of thermal aging on the materials tested. For the current PR-EDB, the peak in the distribution of number of data points versus exposure time is at 2 years, but there are over 100 data points available with over 6 years exposure. For the PR-EDB data, the NRC *Regulatory Guide 1.99* (RG 1.99) predictive equations appear to be valid out to about 9 to 10 years, and although there are few data available, the data out to about 15 years are accurately predicted by RG 1.99. Results of tests for specimens with very low neutron fluence were examined for indications of embrittlement; the data show that the 30-ft-lb shifts are generally less than 20°F. That was also observed for the results from eight thermal capsules with exposure times from about 10,000 to 43,000 h. Both positive and negative shifts were observed but are concluded to be within the scatter expected for shift estimation.

The overview of mechanisms of thermal embrittlement are summarized in the report with a set of related questions: (1) are thermal aging effects possible at low service temperatures, (2) what are the factors involved, and (3) how do radiation and aging effects interact. The answer to the first question appears to be yes, but it may be rarely and is dependent on many factors related to both thermokinetic and micromechanical processes. As to the second question, time and temperature are, of course, intrinsically important. Hardening embrittlement appears to be sensitive to composition, particularly the copper and nickel contents. Additionally, the heat treatment cycles given the steels also appear to be very significant. Of course, the temper embrittlement mechanism associated principally with phosphorus is also a major factor. Of major interest as regards composition effects is, as mentioned earlier, the combination of high copper and high nickel. Preliminary results from UCSB with thermally aged commercial-type steels with high copper and nickel contents, do indicate increased sensitivity to thermal aging in the temperature range of interest. The ultimate question for RPVs, of course, is the third question regarding the interaction of thermal and radiation processes. It is a difficult question to answer and, in general, is intrinsically linked to the effects of neutron flux. Generally, independent aging effects should not be simply added to embrittlement caused by irradiation. Overall, low-flux surveillance data appear to offer an adequate basis to predict embrittlement, although this tentative conclusion must be verified and residual questions regarding flux effects more fully resolved. The postweld heat treatments (PWHTs) given the PNP steam generator and RPV would not be expected to result in significantly different properties.

Regarding the DWT and CVN impact tests on the PNP steam generator welds, the higher-than-expected transition temperatures obtained for the W5214 weld (SG-A) were major factors in suspecting that the weld metal may have experienced thermal embrittlement as a consequence of long-time exposure during operation of the steam generator. It was noted that similar tests on the 34B009 weld removed from a similarly exposed PNP steam generator did not result in unexpectedly high transition temperatures. The nil-ductility transition temperature (NDTT) results for the SG-A weld, although higher than expected based on comparisons with the Combustion Engineering generic weld database, did fall within the range of NDTTs in the database. For DWT tests with low-alloy steels, scatter with a given heat of steel can vary by at least ±20°F. Regarding the use of the now-required one-pass weld technique for fabrication of the brittle crack starter on DWT specimens compared to

the more common two-pass technique used previously, available data for welds are very sparse. Data for six heats of A 533, grade B, class 1 steel, however, showed a maximum difference of 18°F with a mean difference of 4.5°F. The CVN impact data from the SG-A weld and from three other data sets for the W5214 weld were analyzed and compared. The results from these data sets were also compared with another larger data set (Midland Unit 1 weld) for one particular submerged-arc weld. A number of different statistical approaches were examined in these analyses and comparisons. Based on those analyses, the PNP SG-A weld transition temperature is not so far from the average of other estimates for the same weld wire that we would judge the SG-A weld estimate to be significantly different. Additional data for that weld would certainly be helpful, but given the observations on Midland weld compared with those from the four data sets for W5214, it is unlikely that additional measurements would change this conclusion.

During their evaluation of the W5214 weld, CPCO also determined chemical composition at three different depths through the weld thickness, and on three different sections of the steam generator welds. The primary issue addressed in this letter report is that of how the recent PNP steam generator weld chemistry measurements could be used with the previously available data on weld wire heat W5214 to obtain updated average values of the primary elements of interest (Cu, Ni, and P) for this heat of wire. In that regard, the specific results from the SG-A weld analyses were analyzed relative to copper distribution. Because of the fabrication technique used for the steam generator welds, we believe a single average value should be obtained from the 18 new copper measurements made in the 3 weld seams in the PNP steam generator. If a coil-weighted average is used to calculate an average copper value for the W5214 heat, tandem-arc welds should be weighted twice; thus, a weighting factor of six would be applied to the SG-A weld because it used tandem-arc welding and was sampled at three depths. If a weld-weighted average is used, the average composition for each of the various welds in the database should simply be averaged without weighting, and tandem-arc welds should be weighted the same as the single-arc welds. The number of significant digits for the average copper content should be determined within the context of ASTM E29 with consideration of uncertainties in the individual measurements used to obtain the average value. The issue of averaging the copper content for welds which were fabricated with copper-coated weld wire is discussed from a statistical viewpoint, and various strategies for averaging are presented. It is noted that the PNP SG-A weld presents a bimodal distribution of copper, and this observation is discussed relative to weld-to-weld differences and coil-to-coil differences. Based on the statistical tests (t-tests) and the cumulative distributions, there is no statistical justification for combining the SG-A weld copper content data with the existing database for W5214.

12. Technical Assistance for JCCCNRS Working Groups 3 and 12

R. K. Nanstad, S. K. Iskander, M. A. Sokolov, and R. E. Stoller

The purpose of this task is to provide technical support for the efforts of the U.S.-Russian JCCCNRS Working Group 3 on radiation embrittlement and Working Group 12 on aging. Specific activities under this task are: (1) supply of materials and preparation of test specimens for collaborative IAR studies to be conducted in Russia; (2) capsule preparation and initiation of irradiation of Russian specimens within the United States; (3) preparation for, and participation in, working Groups 3 and 12 meetings; and (4) sponsoring of the assignment at ORNL of a scientist from the Russian National Research Center, Kurchatov Institute.

12.1 Irradiation Experiments in Host Country

The CVN and round tensile specimens of two Russian weld metals irradiated in HSSI capsule 10.06 at the University of Michigan FNR have been returned to ORNL. The capsule will be disassembled during the summer of 1995, and testing of the Russian materials is anticipated to be completed prior to the end of 1995.

12.2 Personnel Interactions

The HSSI Program is sponsoring the sabbatical of Dr. Mikhail A. Sokolov at ORNL. Dr. Sokolov's areas of concentration are thermal annealing of irradiated RPV steels and the use of subsize Charpy impact specimens for irradiated studies. The results of his research are presented within the particular technical tasks of HSSI semiannual progress reports and published technical reports and papers.

13. Correlation Monitor Materials

W. R. Corwin

This task has been established with the explicit purpose of ensuring the continued availability of the pedigreed and extremely well-characterized material now required for inclusion in all additional and future surveillance capsules in commercial light-water reactors. Having recognized that the only remaining materials qualified for use as a correlation monitor in reactor surveillance capsules are the pieces remaining from the early HSST plates 01, 02, and 03, this task will provide for cataloging, archiving, and distributing the material on behalf of the NRC. The initial activity to be performed in this task will be to identify existing materials and records in preparation for establishing a storage, monitoring, and disbursement facility.

During this reporting period, concrete was poured and pallets storage racks were installed to provide adequate room for the storage of the correlation monitor material being transferred from its location at the Y-12 Plant to its archival storage location at ORNL. The racks came from surplus material storage at ORNL and hence were obtained at no cost to the HSSI Program. Inquiries into cost-effective means of sheltering the blocks of correlation monitor materials from further weather-related deteriorization were initiated. The most likely approach would be to procure a turn-key sheet metal building installed over the storage racks by an outside contractor to minimize costs.

Most of the material has now been transferred from Y-12 to the ORNL storage area. It has been repositioned on new storage pallets and placed into the storage racks. An update of the detailed material inventory was initiated to ascertain the revised location of all blocks.

Pieces of HSST plate 03 were distributed to participants in the ASTM cross-comparison exercise on subsize specimen testing technology. The use of the HSST 03 will provide for data from the many varieties of tests to be performed to be compared with the standardized data previously developed. The testing techniques will focus on ways to measure transition temperature and fracture toughness.

14. Test Reactor Irradiation Coordination

D. W. Heatherly, I. I. Siman Tov, D. W. Sparks,
E. G. Giles, Jr., and K. R. Thoms

This task was established to supply and coordinate irradiation services needed by NRC contractors other than ORNL. These services include the design and assembly of irradiation capsules as well as arranging for their exposure, disassembly, and return of specimens.

Currently, the UCSB is the only other NRC contractor for whom irradiations are to be conducted. These irradiations will be conducted at the University of Michigan (U. of M.) in conjunction with other irradiations being conducted for the HSSI Program. When this project was initiated, the plan was to modify the current ORNL U. of M. irradiation capsules to facilitate the irradiation of UCSB specimens. The request from UCSB was to have a high, intermediate, and low flux area in which to irradiate their specimen packets and to have the capability of removing and inserting specimen packets at given intervals in order to obtain desired fluences. It was also requested that each area for irradiation of specimen packets have 3 axial temperature zones of 260, 290, and 320°C. Control of the zone temperatures was requested to be within 5°C of desired temperature. After several iterations, it was determined that an entirely new facility and capsule design would be necessary to provide UCSB with the desired fluence, temperature, temperature control, and space for the specimen packets to be irradiated.

The newly developed design consists of a facility that will be located on the east face of the FNR core between two HSSI-IAR facilities. The UCSB facility will be instrumented with heaters and thermocouples for controlling and recording the irradiation conditions of the UCSB specimen packets. The facility has a high-flux area and an intermediate/low-flux area into which baskets of specimen packets can be inserted. The baskets can be removed, disassembled, reassembled, and reinserted into the facility during times when the reactor is shut down. Two baskets will be accommodated by the UCSB facility. The high-flux basket will be inserted into the high-flux area of the facility and will contain a total of 10 UCSB specimen packets within 7 in. of the reactor horizontal midplane. Additional specimen packets can be placed into the uppermost 10 in. of the high-flux basket where the temperature will be controlled at 290°C. This was requested by UCSB for doing irradiations where large flux gradients are not detrimental. The intermediate/low-flux basket will be inserted into the intermediate/low-flux area of the facility and will contain a total of 38 UCSB specimen packets within 7 in. of the reactor horizontal midplane.

During this period, the final design of the facility and specimen baskets was determined through an iterative process involving the designers and thermal analysts. The resulting design should permit the irradiation of all test specimens to within 5°C of their desired temperature. Detailing of all parts is ongoing and should be completed during the next reporting period. Procurement of the facility will also be initiated during the next review period.

CONVERSION FACTORS[a]

SI Unit	English Unit	Factor
mm	in.	0.0393701
cm	in.	0.393701
m	ft	3.28084
m/s	ft/s	3.28084
kN	lb_f	224.809
kPa	psi	0.145038
MPa	ksi	0.145038
MPa•√m	ksi•√in.	0.910048
J	ft•lb	0.737562
K	°F or °R	1.8
kJ/m^2	$in.-lb/in.^2$	5.71015
$W•m^{-3}•K^{-1}$	$Btu/h•ft^2•°F$	1.176110
kg	lb	2.20462
kg/m^3	$lb/in.^3$	3.61273×10^{-5}
mm/N	$in./lb_f$	0.175127
T(°F)=1.8(°C)+32		

[a]Multiply SI quantity by given factor to obtain English quantity.

NUREG/CR-5591
ORNL/TM-11568/V6&N1
Vol. 6, No. 1
Dist. Category RF

INTERNAL DISTRIBUTION

1. D. J. Alexander
2. C. A. Baldwin
3. B. R. Bass
4-14. W. R. Corwin
15. D. F. Craig
16. T. L. Dickson
17. K. Farrell
18. F. M. Haggag
19. H. W. Hayden, Jr.
20. S. K. Iskander
21. J. Keeney
22. E. T. Manneschmidt
23. L. K. Mansur
24. W. J. McAfee
25. D. E. McCabe
26. J. G. Merkle
28. M. K. Miller
29-31. R. K. Nanstad
32. J. V. Pace III
33. W. E. Pennell
34. C. E. Pugh
35. A. F. Rowcliffe
36. R. E. Stoller
37. R. L. Swain
38. K. R. Thoms
40. J. A. Wang
41. ORNL Patent Section
42. Central Research Library
43. Document Reference Section
44-46. Laboratory Records Department
47. Laboratory Records (RC)
48-50. M&C Records Office

EXTERNAL DISTRIBUTION

51. ABB-COMBUSTION ENGINEERING, Windsor, CT 60695

    S. T. Byrne

52. ATI, Suite 160, 2010 Crow Canyon Place, San Ramon, CA 94583

    W. L. Server

53. BABCOCK AND WILCOX, B&W R&D Division, 1562 Beeson St., Alliance, OH 44601

    W. A. Van Der Sluys

54. BETTIS ATOMIC POWER LABORATORY, Westinghouse Electric Corp., P.O. Box 79, West Mifflin, PA 15122

    L. A. James

55. CAROLINA POWER AND LIGHT CO., P.O. Box 1551, Raleigh, NC 27602

    S. P. Grant

56. EG&G IDAHO, INC., P.O. Box 1625, Idaho Falls, ID 83415-2406

V. Shah

57. GROVE ENGINEERING, Suite 218, 9040 Executive Park Drive, Knoxville, TN 37923

W. A. Pavinich

58. HANFORD ENGINEERING DEVELOPMENT LABORATORY, P.O. Box 1970, Richland, WA 99352

M. L. Hamilton

59-60. UNIVERSITY OF CALIFORNIA, Department of Chemical and Nuclear Engineering, Ward Memorial Drive, Santa Barbara, CA 93106

G. E. Lucas
G. R. Odette

61-62. UNIVERSITY OF MICHIGAN, Ford Nuclear Reactor, 2301 Bonisteel Blvd., Ann Arbor, MI 48109-2100

R. Fleming
P. A. Simpson

63. UNIVERSITY OF MISSOURI-ROLLA, Department of Nuclear Engineering, Rolla, MO 65401

A. S. Kumar

64. E. T. Wessel, Lake Region Mobile Home Village, 312 Wolverine Lane, Haines City, FL 33844

65-66. WESTINGHOUSE ELECTRIC CORP., P.O. Box 355, Pittsburgh, PA 15320

W. Bamford
R. C. Shogan

67. WESTINGHOUSE R&D CENTER, 1310 Beulah Rd., Pittsburgh, PA 15325

R. G. Lott

68. DOE OAK RIDGE OPERATIONS OFFICE, P.O. Box 2001, Oak Ridge, TN 37831-6269

Office of Deputy Assistant Manager for Energy Research and Development

69-70. DOE, OFFICE OF SCIENTIFIC AND TECHNICAL INFORMATION, P.O. Box 62, Oak Ridge, TN 37831

71- 200. Given distribution as shown in category RF (NTIS-10)

NRC FORM 335 (2-89) NRCM 1102, 3201, 3202

U.S. NUCLEAR REGULATORY COMMISSION

BIBLIOGRAPHIC DATA SHEET

(See instructions on the reverse)

1. REPORT NUMBER (Assigned by NRC, Add Vol., Supp., Rev., and Addendum Numbers, if any.)

NUREG/CR-5591
Vol. 6, No. 1
ORNL/TM-11568/V6&N1

2. TITLE AND SUBTITLE

Heavy-Section Steel Irradiation Program Semiannual Progress Report for October 1994 Through March 1995

3. DATE REPORT PUBLISHED

MONTH	YEAR
October	1995

4. FIN OR GRANT NUMBER

L1098

5. AUTHOR(S)

W. R. Corwin

6. TYPE OF REPORT

Technical

7. PERIOD COVERED *(Inclusive Dates)*

October 1994 - March 1995

8. PERFORMING ORGANIZATION – NAME AND ADDRESS *(If NRC, provide Division, Office or Region, U.S. Nuclear Regulatory Commission, and mailing address; if contractor, provide name and mailing address.)*

Oak Ridge National Laboratory
Oak Ridge, TN 37831-6285

9. SPONSORING ORGANIZATION – NAME AND ADDRESS *(If NRC, type "Same as above"; if contractor, provide NRC Division, Office or Region, U.S. Nuclear Regulatory Commission, and mailing address.)*

Division of Engineering Technology
Office of Nuclear Regulatory Research
U.S. Nuclear Regulatory Commission
Washington, DC 20555-0001

10. SUPPLEMENTARY NOTES

11. ABSTRACT *(200 words or less)*

The goal of the Heavy-Section Steel Irradiation Program is to provide a thorough, quantitative assessment of effects of neutron irradiation on material behavior, and in particular the fracture toughness properties, of typical pressure vessel steels as they relate to light-water reactor pressure-vessel integrity. Effects of specimen size, material chemistry, product form and microstructure, irradiation fluence, flux, temperature and spectrum, and post-irradiation annealing are being examined on a wide range of fracture properties. The HSSI Program is arranged into 14 tasks: (1) program management, (2) fracture toughness (K_{Ic}) curve shift in high-copper welds, (3) crack-arrest toughness (K_{Ia}) curve shift in high-copper welds, (4) irradiation effects on cladding, (5) K_{Ic} and K_{Ia} curve shifts in low upper-shelf welds, (6) annealing effects in low upper-shelf welds, (7) irradiation effects in a commercial low upper-shelf weld, (8) microstructural analysis of irradiation effects, (9) in-service aged material evaluations, (10) correlation monitor materials, (11) special technical assistance, (12) JPDR steel examination, (13) technical assistance for JCCCNRS Working Groups 3 and 12, and (14) additional requirements for materials. This report provides an overview of the activities within each of these tasks from October 1994 Through March 1995.

12. KEY WORDS/DESCRIPTORS *(List words or phrases that will assist researchers in locating the report.)*

pressure vessels
ductile testing
irradiation
fracture mechanics
cladding
embrittlement
LUS weld metal
crack arrest

13. AVAILABILITY STATEMENT

Unclassified

14. SECURITY CLASSIFICATION

(This Page)

Unclassified

(This Report)

Unclassified

15. NUMBER OF PAGES

16. PRICE